IO, ITS ATMOSPHERE AND OPTICAL EMISSIONS

R. A. BROWN and Y. L. YUNG
Harvard University

Io is surrounded by a halo of atoms which radiate in emission lines. This was discovered by groundbased observations in 1973, a year before Pioneer 10 passed through the Jovian system. Earlier optical and radio observers had reported other anomalies associated with Io, and the Pioneer spacecraft discovered an ultraviolet emission cloud around the satellite and a substantial ionosphere. A new field of planetary research is dedicated to integrating these phenomena into a model of Io and of the Jovian environment with which it strongly interacts.

Sodium dominates the optical emission cloud around Io. The production rate is very large and has not yet been satisfactorily explained. Sputtering by charged particle bombardment may play an important role. The primary excitation mechanism is the resonant scattering of sunlight. While the sodium cloud is brightest near Io, it extends around the entire orbit and is present at low levels in the general Jovian environment. The ionospheric electron density on Io is comparable to that on Mars, a surprising result since the solar flux is much weaker. Here, again, Io's charged particle environment may play an important part. The observed electron profiles plus the constraints provided by the emission cloud are consistent with at least two models of Io's neutral atmosphere.

The four bright satellites of Jupiter have a unique perennial interest and historical importance. Their discovery by Galileo in 1610 was among the very first achievements of the telescope. Early observers intensively chronicled Io's rapid synodic motion—and this was to a very practical purpose, since it established an accurate and accessible timepiece. By comparison with local solar time, terrestrial longitude could be measured. In the late seventeenth century Römer found an annual phase lag in "Io time" and first determined the finite speed of light.

Modern studies of the Galilean satellites focus on their physical properties. Interest has been sparked by the view that the Jovian system may be a textbook in microcosm of the solar system. The observational record, especially for Io, is replete with startling discoveries. Among them are a possible post-eclipse brightening (Binder and Cruikshank 1964) and a modulation of

Jovian decametric radiation (Bigg 1964). Recently we have learned that Io is a source of atomic resonance line emission and that it possesses a substantial ionosphere and therefore an atmosphere. These phenomena are related, and our current understanding of them and their relationship is reviewed here.

The chapter is divided into two parts. The first is primarily observational, and its focus is on measurements of the line emission from Io and its environment. The second part is primarily theoretical, and it deals with current models of Io's atmosphere. No single existing theory satisfactorily treats all the processes which are thought to be important; however, a variety of models for Io's surface and environment have been developed in the context of recent observational data (McElroy and Yung 1975; Matson *et al.* 1974; Macy and Trafton 1975).

In Sec. I the sodium D-line measurements are documented and set in their observational context. Section II reviews Pioneer 10's observation of an ultraviolet emitting region associated with Io, which is probably a cloud of atomic hydrogen. Section III reports on the current state of the search for other line emissions. Section IV discusses future observational work.

In Sec. V we discuss the ionosphere and conclude that the atmosphere may be cooler than the observed sodium and that the exobase probably stands well above Io's surface. In Sec. VI we discuss possible sources of hydrogen; its escape into the surrounding space is not a problem. In Sec. VII we treat the alternative sources of sodium; its escape *is* a problem. Having motivated the observational constraints on the neutral atmosphere, in Sec. VIII we show that two different models are consistent with the observations.

I. SODIUM LINE EMISSION FROM IO

The observation of sodium D-line emission associated with Io was first made by Brown in 1973 (see Brown 1974). A Doppler shift analysis of a high-resolution spectrum positively identified Io as the source. Only Io of the four Galilean satellites showed D-line emission to the limit of the instrumental sensitivity. The strong emission varied with large amplitude on a short time scale, and was possibly correlated with Io's orbital position.

The sodium phenomenon has been intensively observed during the 1973 and 1974 oppositions of Jupiter, but it is still rather poorly understood. Beyond its existence, the only unambiguous facts are that the emission also comes from the neighboring space around Io (Trafton *et al.* 1974) and that the brightness of the sodium nearest Io is definitely correlated with the satellite's orbital phase angle measured from superior heliocentric conjunction (Bergstralh *et al.* 1975). The observational challenge, somewhat simplified, is to record the characteristics of a spatial continuum which is a spectral point-source in the presence of a spectral continuum which is a spatial point-source. The former (the sodium cloud) and the latter (Io) also undergo tem-

poral variations with regard to observational perspective and brightness. Therefore, it is important for this chapter to set the sodium measurements in their observational context. The first three subsections lay that groundwork. In A we discuss the sunlight incident on Io and reflected from its surface. In B we characterize and label the spatial regimes relevant to the observational problem. In C we review some fundamental physics of the sodium atom which relates directly to the D-line observations.

In D the dominant excitation mechanism for the D-line emission is established by reviewing the observations and conclusions of Bergstralh *et al.* (1975). That mechanism is solar resonant scattering, and its recognition is important for interpreting the high resolution spectra and photometric studies discussed in E. In F we discuss low-intensity sodium emission recorded in the Jovian environment remote from Io.

A. Incident and Reflected Solar Light Near the D-Lines

The solar radiation incident on the Jupiter system has direct importance to the optical observations of Io's sodium in two ways. First, this light is resonantly scattered by free atoms of sodium. The relevant quantity for studying this phenomenon is the amount of solar radiation available for scattering, that is, falling within the D_1 and D_2 absorption coefficient profiles for a certain Doppler shift of the sodium with respect to the sun. Second, the solar light reflected from Io's surface serves to calibrate measurements of the sodium emission photometrically. For that procedure the important quantity is the flux at Earth from Io in the vicinity of the D-lines. We call this quantity πF_I (.59), and it refers to the continuum flux from Io at 0.59 μm between Fraunhofer absorption lines.

The solar spectrum near the D-lines at $\lambda_{D_2} = 5889.95$ Å and $\lambda_{D_1} = 5895.92$ Å is marked by deep and broad absorptions due to sodium in the sun. A high-resolution, photometric spectrum of the light from the whole solar disc has been obtained and reduced by C. D. Slaughter of Kitt Peak National Observatory. It has been published by Parkinson (1975) and is reproduced in Fig. 1 and Table I. The Doppler shift due to the relative motion with respect to the sun determines the points on the D_1 and D_2 solar absorption lines which can excite sodium in Io's environment. The range of Doppler shifts associated with Io's orbital motion (17.3 km sec^{-1}) is about $\pm$ 0.34 Å.

Referring to the observational geometry shown schematically in Fig. 2, the Io-Sun Doppler shift is proportional to sin (θ_{SHC}) except for a small correction due to Jupiter-Sun motion. The tabulated values, γ_{D_1} and γ_{D_2}, are fractions of $\pi F_\odot$ (.59), the incident solar flux in the nearby continuum. The ratio $\gamma_{D_2}/\gamma_{D_1}$ remains remarkably steady at about 0.85 over the range sampled by Io.

$\pi F_\odot$ (.59) can be obtained by a wavelength interpolation in a table of mean solar disc intensities (Allen 1973), $F_\odot'$ (λ), which refers to the continuum between lines

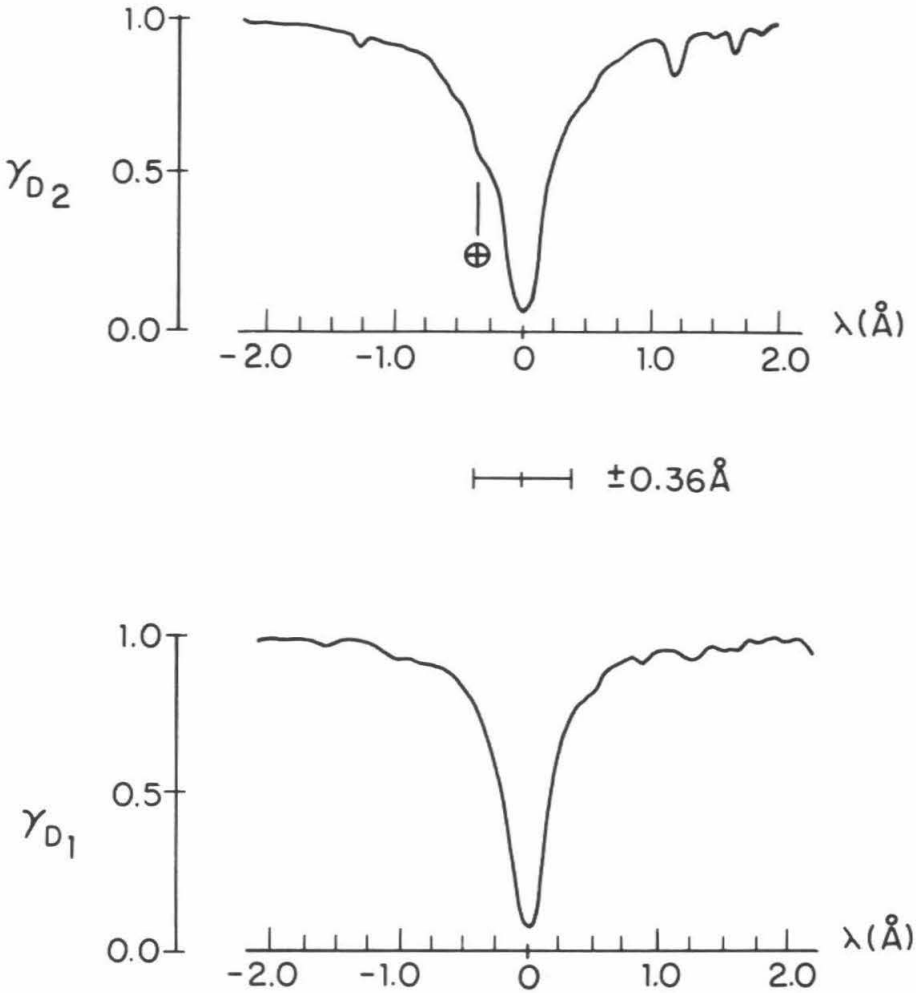

Fig. 1. The solar spectrum in integrated light in the regions of the sodium D_2 and D_1 Fraunhofer lines (obtained by C. D. Slaughter). The horizontal bar shows the region tabulated in Table I and indicates the regions of interest for the Io problem. In the D_2 spectrum there are several telluric H_2O lines, the largest of which is marked and none of which have been removed (From Parkinson 1975).

$$\pi F_{\odot}(.59) = \pi F_{\odot}'(.59)\left(\frac{R}{r}\right)^2 = 5.9 \times 10^{13}\,\frac{1}{r^2}\ \text{photon cm}^{-2}\ \text{Å}^{-1}\ \text{sec}^{-1} \qquad (1)$$

where R is the solar radius and r is the Jupiter-Sun distance measured in A.U. At "mean opposition," $r = a \equiv 5.203$ A.U., and

$$\pi F_{\odot}^{m.o.}(.59) = 2.02 \times 10^{12} \text{ photon cm}^{-2} \text{ Å}^{-1} \text{ sec}^{-1}. \quad (2)$$

πF_I (.59) is derived from measurements of the flux, πF_I (V), from Io in the V-spectral pass-band which have been recently reviewed by Morrison and Morrison (1976). The V-filter is 90 Å wide, and the effective wavelength for Io's color is about 0.55 μm. Io's flux is expressed in terms of the absolute calibration of the V-magnitude system:

$$\pi F_I(V) = \pi F_0(V)^{-0.4 V_I} \quad (3)$$

where $\pi F_0(V) = 3.72 \times 10^{-9}$ erg cm^{-2} sec^{-1} Å^{-1} (Allen 1973). V_I is Io's V-magnitude, which varies with all four independent parameters defining the observational geometry. Dependence on r and Δ is simply inverse-square. A strongly backscattering phase function with an "opposition surge" in brightness is embodied in the α-dependence: Io is 50% brighter at opposition than at maximum solar phase angle (referred to the same Earth-Io separation). A periodic variation with orbital phase angle θ_{SGC} has an amplitude of 8% and implies synchronous rotation of the satellite. Figure 3*a* shows V_I (α), which is referred to "mean opposition" distances, $r = a$ and $\Delta = a - 1$. Shown in Fig. 3*b* is the nominal variation of Io's magnitude with rotational phase, δV_I (θ_{SGC}). These data are taken from the Morrisons' paper, and the result is that πF_I (V) can be computed with a few percent uncertainty for the time of a particular observation:

$$V_I = V_I(\alpha) + \delta V_I(\theta_{SGC}) + 5 \log\left(\frac{r\Delta}{a(a-1)}\right). \quad (4)$$

Using πF_I (V), πF_I (.59) can be determined by accounting for Io's color.

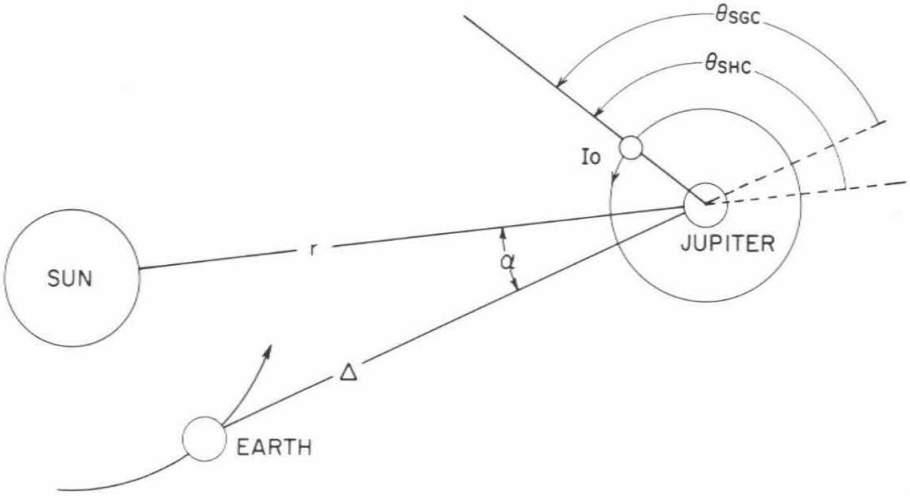

Fig. 2. The geometry of groundbased observations of Io.

TABLE I

The solar spectrum in integrated light near the D lines. The height of the spectrum is given as a fraction of the continuum height.[a]

Δλ(mÅ)	γ_{D_2}	γ_{D_1}	Δλ(mÅ)	γ_{D_2}	γ_{D_1}	Δλ(mÅ)	γ_{D_2}	γ_{D_1}
360	.6298	.7315	100	.1898	.2409	− 110	.2266	.2828
50	.6195	.7256	90	.1591	.1986	− 20	.2617	.3239
40	.6095	.7176	80	.1312	.1601	− 30	.2951	.3616
30	.5995	.7091	70	.1069	.1276	− 40	.3252	.3948
20	.5893	.6995	60	.0872	.1022	− 50	.3513	.4233
10	.5786	.6889	50	.0727	.0841	− 60	.3736	.4478
300	.5672	.6777	40	.0629	.0719	− 70	.3929	.4691
90	.5552	.6661	30	.0566	.0641	− 80	.4101	.4883
80	.5426	.6542	20	.0527	.0592	− 90	.4256	.5061
70	.5296	.6417	10	.0503	.0564	− 200	.4394	.5229
60	.5170	.6281	5	.0495	.0557	− 10	.4517	.5389
50	.5051	.6139	0	.0490	.0555	− 20	.4633	.5541
40	.4942	.5991	− 5	.0489	.0558	− 30	.4747	.5687
30	.4836	.5840	− 10	.0491	.0566	− 40	.4858	.5832
20	.4725	.5685	− 20	.0510	.0597	− 50	.4963	.5977
10	.4602	.5524	− 30	.0549	.0650	− 60	.5060	.6119
200	.4466	.5353	− 40	.0612	.0733	− 70	.5155	.6259
90	.4317	.5169	− 50	.0706	.0858	− 80	.5246	.6396
80	.4155	.4974	− 60	.0843	.1041	− 90	.5320	.6531
70	.3975	.4763	− 70	.1035	.1291	− 300	.5357	.6662
60	.3768	.4532	− 80	.1283	.1609	− 10	.5360	.6789
50	.3524	.4274	− 90	.1582	.1986	− 20	.5361	.6910
40	.3237	.3979	− 100	.1915	.2401	− 30	.5410	.7025
30	.2913	.3641				− 40	.5538	.7136
20	.2870	.3259				− 50	.5729	.7241
110	.2226	.2842				− 360	.5940	.7339

[a]These data are shown graphically in Figure 1 and are from Parkinson (1975).

The spectral reflectivity studies of Johnson and McCord (1970) show Io to be 6% brighter at 0.59 μm than at 0.55 μm:

$$\pi F_I\,(.59) = 1.06\ \pi F_I\,(V)\,.$$

As an illustration, we consider the case of a "mean" opposition and neglect the effect of orbital phase.

$$V_I^{m.o.} = 4.84\,. \tag{5}$$

Then

$$\pi F_I^{m.o.}\,(.59) = 12.9 \text{ photon cm}^{-2}\ \text{Å}^{-1}\ \text{sec}^{-1}\,. \tag{6}$$

Given Io's size, $R_I = 1830$ km, and the incident solar flux, the value of πF_I (.59) is extraordinarily high for all observing geometries. This is illustrated by the geometric albedo

$$p(.59) = \frac{\pi F_I^{m.o.}(.59)}{\frac{1}{\pi} \cdot \pi F_\odot^{m.o.}(.59) \cdot \frac{\pi R_I^2}{(a-1)^2}} = 0.75 . \tag{7}$$

Another relevant dramatization of Io's brightness is the comparison of πF_I (.59) to the flux πF_ℓ which would be observed from a white Lambert sphere exactly replacing Io in size and position. Ignoring the orbital phase modulation, the ratio πF_I (.59)/πF_ℓ varies from 1.1 to 0.7 as the solar phase angle varies from 0° to the maximum of 12°. We shall discuss below in D the peculiar significance of this effect for sodium observations; it makes sodium in Io's atmosphere difficult to observe from Earth.

B. The Spatial Domains

Io is not a point source; its diameter subtends 1.2 arc-seconds at opposition and 0.8 arc-seconds at conjunction with the sun. Under typical observing conditions, "seeing" further spreads Io's radiation into a peaked distribution two or more arc-seconds full-width at half-maximum (*FWHM*). This distribution is Io's continuum surface brightness, and its integral over solid angle is the continuum flux. To the extent that the surface brightness is approximated by a Gaussian distribution of angular size σ arcsec *FWHM*, the central intensity is

$$J_0(\lambda) = 3.75 \times 10^{10} \left(\frac{\pi F_I(\lambda)}{\sigma^2}\right). \tag{8}$$

This result can be expressed as an apparent emission rate[1] for the center of the seeing distribution if πF_I (λ) has the units photon cm^{-2} sec^{-1} Å^{-1}

$$E_0(\lambda) = 0.472\left(\frac{\pi F_I(\lambda)}{\sigma^2}\right) \text{ MR Å}^{-1} . \tag{9}$$

Continuing the illustration in the previous section, at opposition the apparent emission rate in the center of a Gaussian seeing disc 2 arcsec *FWHM* is 1.5 MR Å^{-1}.

For discussion purposes, the sodium in Io's vicinity can be partitioned into three regions. Region *A* is spatially coincident with Io's visible disc and corresponds to sodium in Io's bound atmosphere. Region *B* has direct association with Io and extends 5 – 15 arcsec from it; this is the sodium cloud first identified by Trafton. Extremely faint D-line emission has been reported extending many arcmin away from Io, originating in remote parts of Io's orbit and beyond, by Wehinger and Wyckoff (1974), Mekler and Eviatar (1974) and Mekler *et al.* (1975). This is Region *C*.

---

[1]Apparent emission rate (E) = $4\pi \times 10^{-6} J$, where J is the measured surface brightness in photons sec^{-1} cm^{-2} ster^{-1} (Appendix II of Chamberlain 1961). E is measured in Rayleighs, and kR and MR are 10^3 and 10^6 Rayleighs respectively. The qualifier "apparent" is used because E is equal to a column emission rate only for an optically thin cloud. The term is also commonly used in optically thick situations.

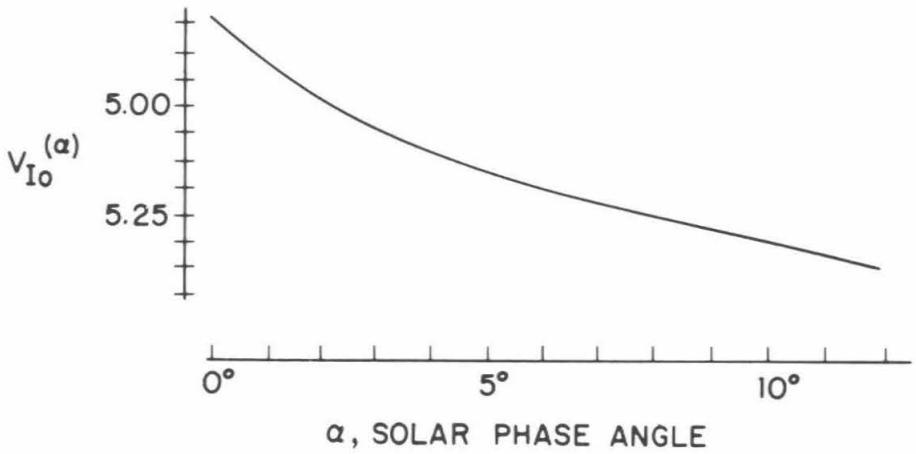

Fig. 3*a*. The dependence of Io's magnitude on the solar phase angle (Morrison and Morrison 1976).

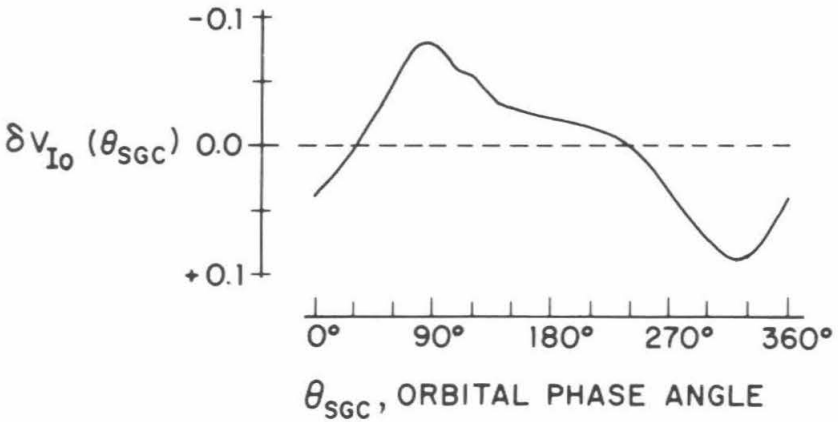

Fig. 3*b*. The dependence of Io's magnitude on the orbital phase angle (Morrison and Morrison 1976).

The observability of these regions is determined by both their brightness and their contrast with the background. For Region *A* that background is the bright disc of Io, and the contrast is poor if a resonant scattering mechanism alone excites the sodium in Io's atmosphere. This point is discussed below in D. For Regions *B* and *C* the backgrounds are the telluric sodium nightglow and the halos of scattered continuum radiation from Jupiter and its satellites. The former is substantially fainter even than Region *C*, and

it is observationally distinguishable from D-line radiation originating in the Jovian system: it exhibits no Doppler shift and is spatially uniform over the telescopic field. The scattered continuum radiation is a serious impediment to observations at spectral resolution lower than ~ 10,000. As discussed in Sec. IV. this has prevented imaging the sodium cloud with conventional techniques. The apparent emission rate of Region *B* is tens of kR. Absolute photometry of Region *C* has not been reported, but a comparison of the detections with the 5577 Å line in the telluric airglow implies an apparent emission rate less than one kR. The distinction between Regions *B* and *C* is drawn on the basis of existing observations which do not manifest the transition from one region to the other. The demonstration that the distinction is artificial, or the definition of the boundary between Regions *B* and *C*, awaits further study.

Since the bulk of the existing sodium observations have been made with astronomical slit spectrographs, some specific remarks are in order about the reduction of such spectra. A usual procedure is to record a spectrum of Io itself and to use the instrumental response to Io's reflected solar continuum to calibrate sodium emission spectra. If the entire disc of Io passes through the entrance aperture, the recorded spectral continuum near the D-lines will be the instrumental response to πF_I (.59). Since spectral and spatial resolution are not independent for these instruments, however, some fraction of Io's continuum image is lost on the slit jaws during observations which press for higher spectral resolution. In such cases, the distribution of Io's continuum surface brightness must be modeled in its projection on the slit, for only by knowing the actual number of photons incident on the detector is it possible to calibrate the system's response. This point would be academic if the emission came only from Region *A*, since the effects of seeing and truncation by the slit jaws would affect continuum and emission identically. But this is not the case for Io, and the analyses of spectra taken with Io in the spectrograph slit depend on hypotheses about the spatial distributions of the continuum and emission components (see e.g., Brown *et al.* 1975).

C. *Atomic Physics of the Sodium D-Lines*

The sodium D-lines[2] are transitions between the ground state ($3s^2S_{\frac{1}{2}}$) and the first excited state which is split by spin-orbit coupling into two fine structure components ($3p^2P_{\frac{1}{2}}$, $3p^2P_{\frac{3}{2}}$). The positions and oscillator strengths of the lines are:

$$\begin{array}{lll} \lambda_{D_1} = 5895.92\ \text{Å} & \nu_{D_1} = 16956.183\ \text{cm}^{-1} & f_{D_1} = 0.327 \\ \lambda_{D_2} = 5889.95\ \text{Å} & \nu_{D_2} = 16973.379\ \text{cm}^{-1} & f_{D_2} = 0.655 \end{array} \qquad (10)$$

[2]For a review of the physics of the sodium atom with special emphasis on observations of the telluric sodium airglow, see Chamberlain (1961).

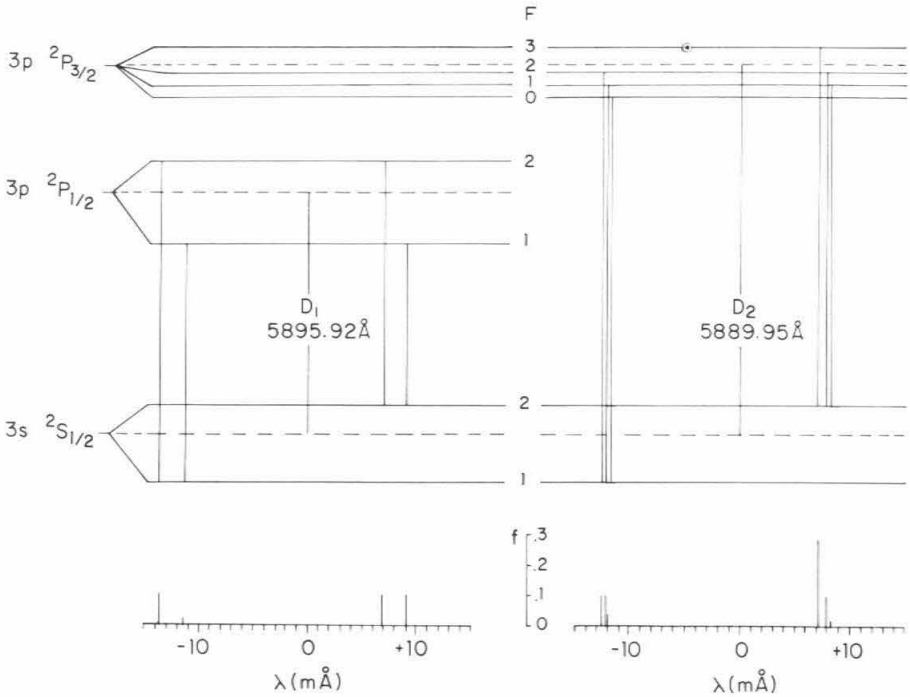

Fig. 4. A schematic representation of the energy levels in atomic sodium between which the D-lines originate. The wavelengths of the centroids λ_{D_1} and λ_{D_2} are given. Allowed transitions are indicated by lines connecting the appropriate sublevels. For each component the oscillator strength position and the wavelength position relative to the centroid is shown below.

The only stable isotope of sodium is $_{11}Na^{23}$ with nuclear spin $I = \frac{3}{2}$. Hyperfine structure results from the coupling between the nuclear spin **I** and the total electronic angular momentum **J** to produce $\mathbf{F} = \mathbf{I} + \mathbf{J}$. The resultant F-manifolds and the allowed transitions ($\Delta F = \pm 1, 0$) are illustrated in Fig. 4. Table II gives the oscillator strengths of these hyperfine transitions and their wavelength positions with respect to the D_1 and D_2 centroids, λ_{D_1} and λ_{D_2}.

For each hyperfine transition, the absorption coefficient of an individual atom at rest is distributed over wavelength in a Lorentz line shape with full-width at half-maximum $\Delta\nu_L = 3.10^{-4}$ cm^{-1} or $\Delta\lambda_L = 0.1$ m Å. The integral of this distribution is

$$\alpha(F_s, F_p) = \frac{\pi e^2}{mc} f(F_s, F_p) \tag{11}$$

which has units of cm^2 sec^{-1}.

TABLE II[a]

The Oscillator Strengths and the Wavelength Positions of the D_1 and D_2 Hyperfine Components

		$^2P_{\frac{1}{2}}$	
	D_1	$F = 1$	$F = 2$
$^2S_{\frac{1}{2}}$	$F = 1$	0.020 − 11.4 mÅ	0.102 − 13.6 mÅ
	$F = 2$	0.102 + 9.1 mÅ	0.102 + 6.9 mÅ

		$^2P_{\frac{3}{2}}$			
	D_2	$F = 0$	$F = 1$	$F = 2$	$F = 3$
$^2S_{\frac{1}{2}}$	$F = 1$	0.041 − 12.0 mÅ	0.102 − 12.2 mÅ	0.102 − 12.6 mÅ	——
	$F = 2$	——	0.020 + 8.3 mÅ	0.102 + 7.9 mÅ	0.287 + 7.2 mÅ

[a]These transitions are shown schematically in Fig. 4.

For an ensemble of atoms in thermal motion, the absorption coefficient per atom is the convolution of the Lorentzian with a Doppler (Gaussian) profile with *FWHM*

$$\Delta\nu_d = 2.5 \times 10^{-3} \sqrt{T} \text{ cm}^{-1}, \tag{12}$$

or

$$\Delta\lambda_d = 7.16 \times 10^{-7} \lambda \sqrt{\frac{T}{23}} \approx 0.88 \sqrt{T} \tag{13}$$

where T is the temperature in °K and the unit is 10^{-3} Ångstrom. For naturally occurring temperatures, then, the absorption coefficient per atom of the hyperfine line (F_s, F_p) is effectively distributed in the Doppler profile

$$\alpha_\nu(F_s, F_p) = \left(\frac{\pi e^2}{mc}\right) f(F_s, F_p) \frac{2(\ln 2)^{\frac{1}{2}} c}{\sqrt{\pi}\, \Delta\nu_D} \exp\left[-\left(\frac{\nu - \nu(F_s, F_p)}{\Delta\nu_d}\right)^2 \ln 2\right] \tag{14}$$

or, written as a function of wavelength,

$$\alpha_\lambda(F_s, F_p) = \left(\frac{\pi e^2}{mc}\right) f(F_s, F_p) \frac{2(\ln 2)^{\frac{1}{2}}}{\sqrt{\pi}\, \Delta\lambda_D} \exp\left[-\left(\frac{\lambda - \lambda(F_s, F_p)}{\Delta\lambda_D}\right)^2 \ln 2\right]. \tag{15}$$

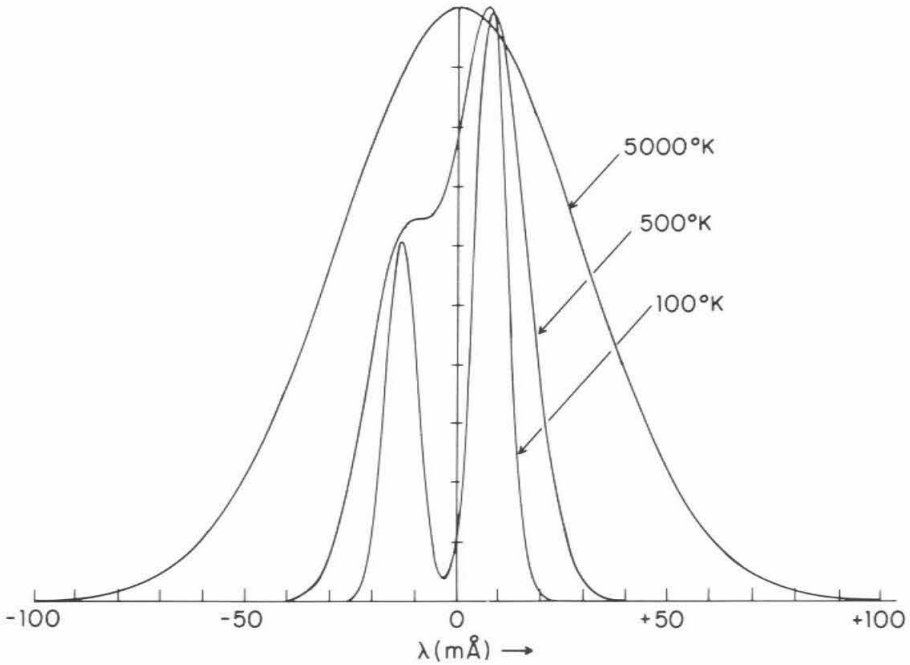

Fig. 5. The theoretical D_1 absorption coefficient as a function of wavelength relative to the centroid λ_{D_1} for sodium kinetic temperatures 100, 500 and 5000°K. The profiles have been normalized to the same maximum height.

The absorption coefficient profiles per atom are the sums of $\alpha_\lambda(F_s, F_p)$ or $\alpha_\nu(F_s, F_p)$ over the allowed transitions, assuming the states F_s are populated according to their multiplicity:

$$\alpha_\nu = \sum_{F_s, F_p} \alpha_\nu(F_s, F_p) \tag{16}$$

and likewise for α_λ.

The shape of the D_1 absorption coefficient as a function of wavelength is shown in Fig. 5 for 100, 500 and 5000°K. Only for temperatures higher than a few thousand degrees are the D-lines adequately described by a single component of strength f_{D_1} or f_{D_2} distributed in a Gaussian $\Delta\lambda_d$ $FWHM$ centered on λ_{D_1} or λ_{D_2}.

Non-thermal mechanisms may produce a velocity dispersion in the atoms sampled by a particular observation of Io's sodium cloud (Matson *et al.* 1974; Trafton and Macy 1975). If thermodynamic equilibrium does not apply, the absorption coefficients cannot be characterized by a single temperature, and the fundamental quantity is the detailed distribution of atomic velocities.

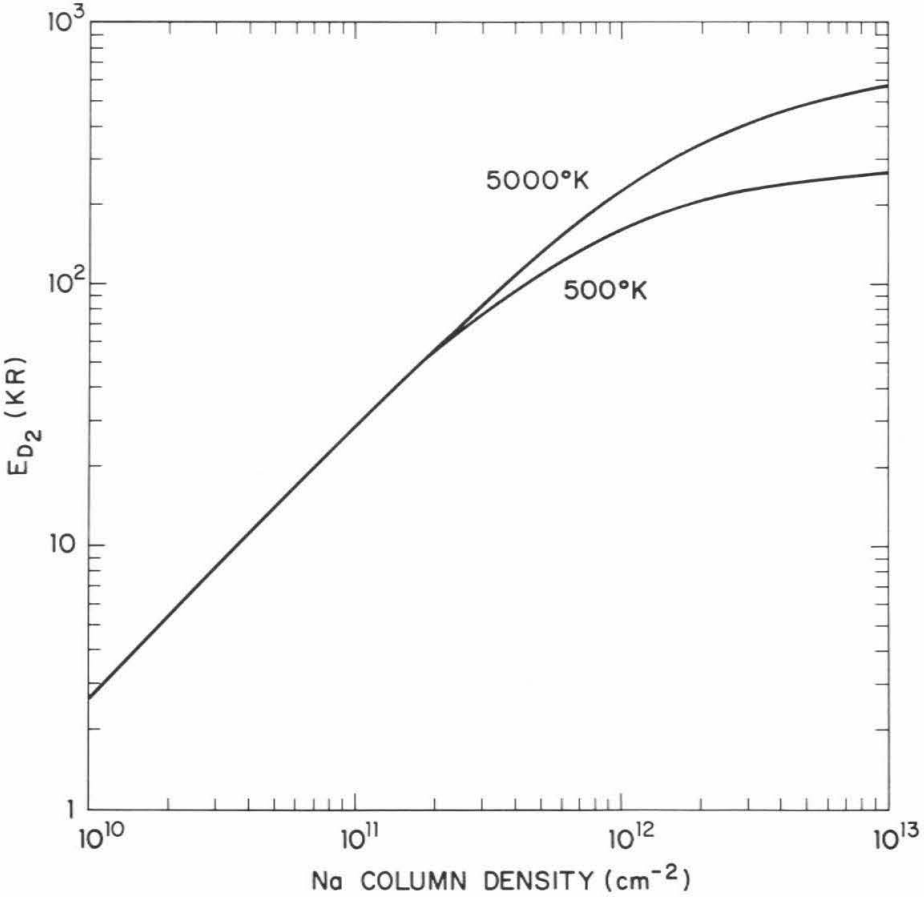

Fig. 6*a*. Intensity of sodium D_2 emission versus sodium column abundance for 500 and 5000°K. The continuum solar flux is taken to be 2.02×10^{12} photons cm^{-2} sec^{-1} $Å^{-1}$, and $\gamma_{D_2} = 0.61$.

Combining the work above with that in Subsections A and B, we may set the physical scale of the interaction of sodium with solar flux in Io's environment. Anticipating an observational result discussed below in E, we consider a sodium cloud with column abundance N atoms cm^{-2} which is sufficiently "hot" to ignore hyperfine structure. The optical depth in the center of the D_1 line is then

$$\tau_{D_1} = \alpha_{\nu_{D_1}} N = 1.1 \times 10^{-10} T^{-\frac{1}{2}} N , \tag{17}$$

while τ_{D_2} is twice as great. The column abundance corresponding to unit optical depth at 5000°K is 6.6×10^{11} atoms cm^{-2}.

If Io's sodium cloud is optically thin, its apparent emission rate due to the resonant scattering of solar flux in a D-line may be estimated as follows.

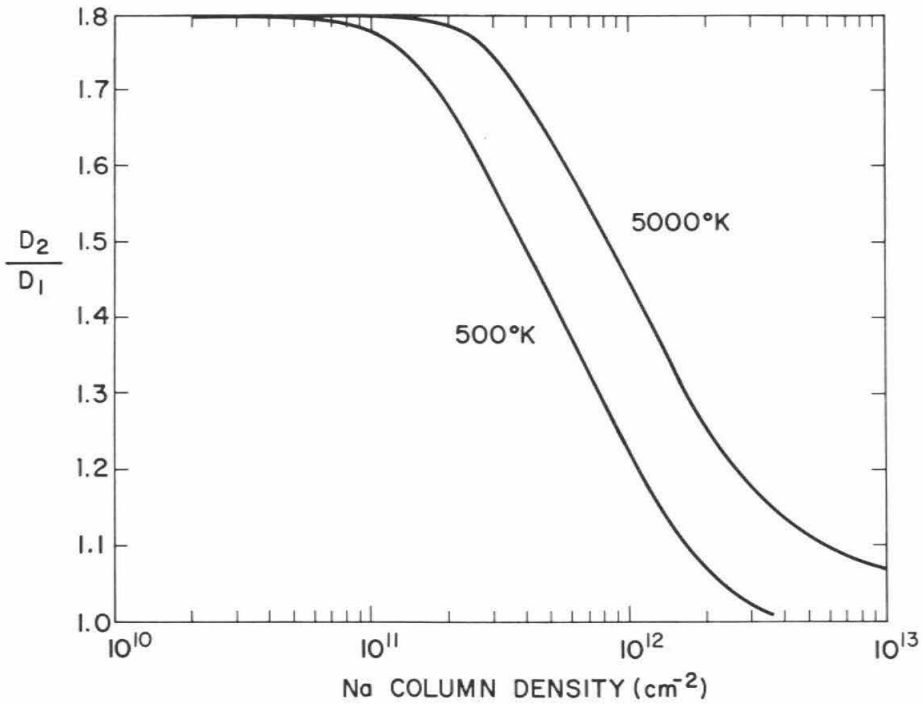

Fig. 6*b*. Ratio of emergent D_2 to D_1 apparent emission rates for 500°K and 5000°K. γ_{D_2} and γ_{D_1} are taken to be 0.61 and 0.72 respectively.

[Here the reader is again referred to Chamberlain (1961).] For plane-parallel geometry and zero solar phase angle

$$E = gN \tag{18}$$

where the g-factor is given by

$$g \equiv \left[\gamma \cdot \pi F_{\odot}(.59) \cdot \frac{\lambda^2}{c}\right] \frac{\pi e^2}{mc} f. \tag{19}$$

For the D_1 line

$$E_{D_1} \equiv 0.20\, \gamma_{D_1}\, N\,. \tag{20}$$

As an example, take $\gamma_{D_1} = 0.5$ and $N = 10^{11}$ atoms cm^{-2}, then

$$E_{D_1} \equiv 10\,\mathrm{kR}\,. \tag{21}$$

As the column abundance of sodium increases, a detailed radiative transfer calculation is required to compute E as a function of temperature and optical thickness. The gross effect is that the D_2/D_1 ratio is reduced and the emission line profiles are broadened due to saturation in the line core. These

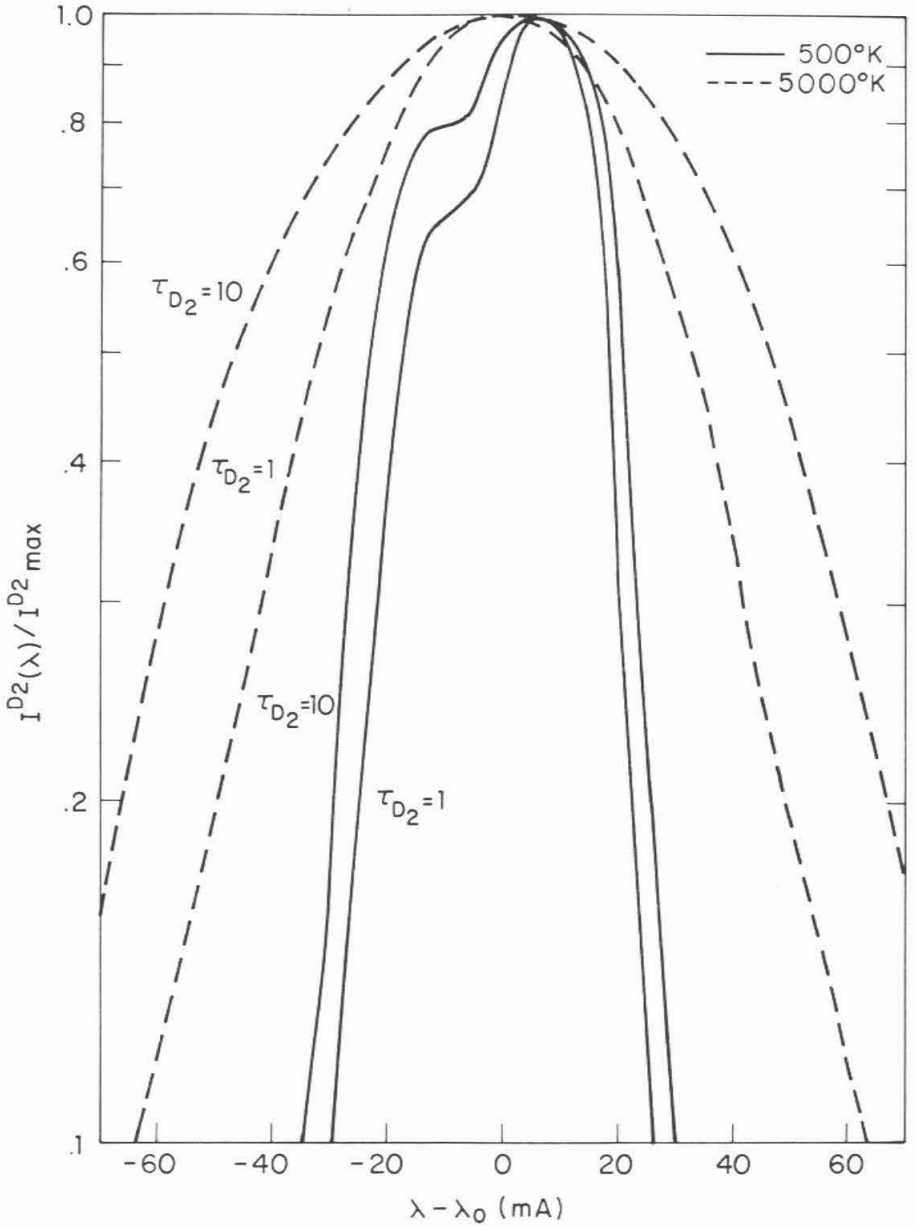

Fig. 6c. Profiles of the emergent D_2 line co-normalized to the same peak intensity.

effects are illustrated in Fig. 6 which shows E_{D_2}, D_2/D_1 and the D_2 emission line profile versus column abundance for a sodium cloud. These results are taken from McElroy and Yung (1975) and include modifications for hyper-

fine structure and the Rayleigh phase function in some components of the D_2 line, suggested by Macy (personal communication).

D. The D-Line Excitation Mechanism

The early D-line observations of Brown (1974) included some very high emission fluxes from Io: several Ångstroms equivalent width for $D_1 + D_2$ when a spectrometer of large spatial aperture was used. The corresponding apparent emission rates were tens of MR if the emission came from Region *A* and impossibly high to explain by solar resonant scattering. On this basis, the first theory of the D-line excitation, proposed by McElroy *et al.* (1974), suggested an auroral mechanism involving a resonant transfer of energy to the sodium atoms from vibrationally excited N_2. Such a mechanism had been suggested by Hunten (1965) to account for D-line emission in terrestrial aurorae. In addition to explaining the high intensities, this model was attractive in that it was specific to the D-lines (no other emissions had been discovered) and could explain the broadened lines seen by Brown and Chaffee (1974), which are discussed below.

Figure 7 shows a spectrum from Trafton *et al.* (1974) illustrating the discovery that the sodium emission extends into space beyond Io. The circular aperture of the spectrometer was 4.7 arc-seconds in diameter, and it was set on the sky next to Io as shown. The recorded apparent emission rates were $E_{D_1} = 7.6 \pm 0.5$ kR and $E_{D_2} = 14.6 \pm 0.5$ kR, with $D_2/D_1 = 1.9 \pm 0.2$. This is Region *B* by the definitions in Sec. I.B, and its recognition led directly to the suggestion that resonant scattering of sunlight is indeed the emission mechanism (Trafton *et al.* 1974; Matson *et al.* 1974). The work presented in Sec. I.C shows that these intensities and their ratio are consistent with sunlight being scattered from an optically thin sodium layer. The anomalously high emissions from Io seen by Brown (1974) can be understood if this emission covered an area within 10–15 arcsec of Io.

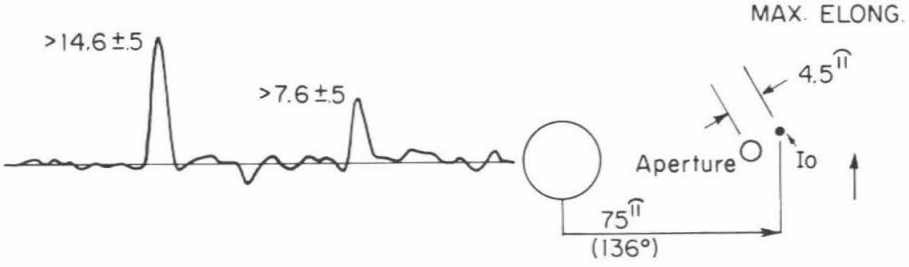

Fig. 7. A D-line spectrum of Region *B* from Trafton *et al.* (1974). The apparent emission rates in kR for the D_1 and D_2 lines are shown, and $D_2/D_1 = 1.9 \pm 0.2$. The observing geometry is shown schematically on the right. θ_{SOE} is shown in parenthesis. The elongation point is indicated with an arrow.

Bergstralh *et al.* (1975) measured the brightness of Io's sodium emission almost nightly in July and August of 1974. The measurements were all taken with the same instrumental arrangement and were reduced identically. The 3×8 arcsec spectrograph aperture was centered on Io, recording all Io's continuum flux plus emission from a definite portion of the surrounding space. The consistency of the observational technique clearly revealed the time signature of the resonant scattering mechanism: the variation of the emission in direct proportion to the amount of sunlight available for scattering at the appropriate Doppler-shifted D-line wavelengths (see Fig. 1). Figure 8 shows the observations and their fit to the predictions of the scattering theory. The departures of the cloud intensity from simple direct proportion to the insolation are possibly attributable to an asymmetrical sodium distribution and the varying observational perspective, which produce varying optical thickness along the line of sight as defined by the projection of the spectrograph aperture on the sky.

Evidence against any residual auroral mechanism is the absence of anomalies which could be attributed to an emission core from Region *A*. An upper limit of $\sim$ 130 kR is set by Bergstralh *et al.* (1974) to such constant additional source. This result is supported by the absence of $\gtrsim$ 2 kR emission during or near solar eclipse on Io; null findings have been obtained by a number of observers including Macy and Trafton (1975).

If the *only* D-line excitation mechanism is solar resonant scattering, then an important conclusion can be drawn: sodium in Region *A* is virtually unobservable from Earth. This was first pointed out by Brown *et al.* (1975). The reason for this curiosity is that there is very low contrast between Io's bright surface and sodium atoms in the atmosphere of Io. Those atoms scatter solar photons nearly isotropically [see the discussion by Parkinson (1975)], so that an optically thick sodium layer close around Io in Region *A* will have nearly the phase function of a Lambert sphere in scattering D-line photons. But Io's surface itself returns to us approximately as much reflected solar light as a Lambert sphere in that whole wavelength range (see Sec. I.A). Since the terrestrial observer cannot distinguish between a photon scattered from Io's surface and one scattered by a sodium atom in Region *A*, it is difficult to detect that sodium by looking for excess brightness in the D-lines.

E. Physical Measurements of the Region B *Sodium Cloud*

The D_1 and D_2 line emissions from Io are sufficiently broad to be resolved with high resolution astronomical spectrographs. This was first reported by Brown and Chaffee (1974). Spectra at higher resolution have been reported and analyzed by Macy and Trafton (1975) and Brown *et al.* (1975). Accounting for instrumental broadening, the recorded lines measure about 60–80 m Å *FWHM*. All of the spectra were recorded with Io in the spectrograph slit and the continuum was subtracted to isolate the emission fea-

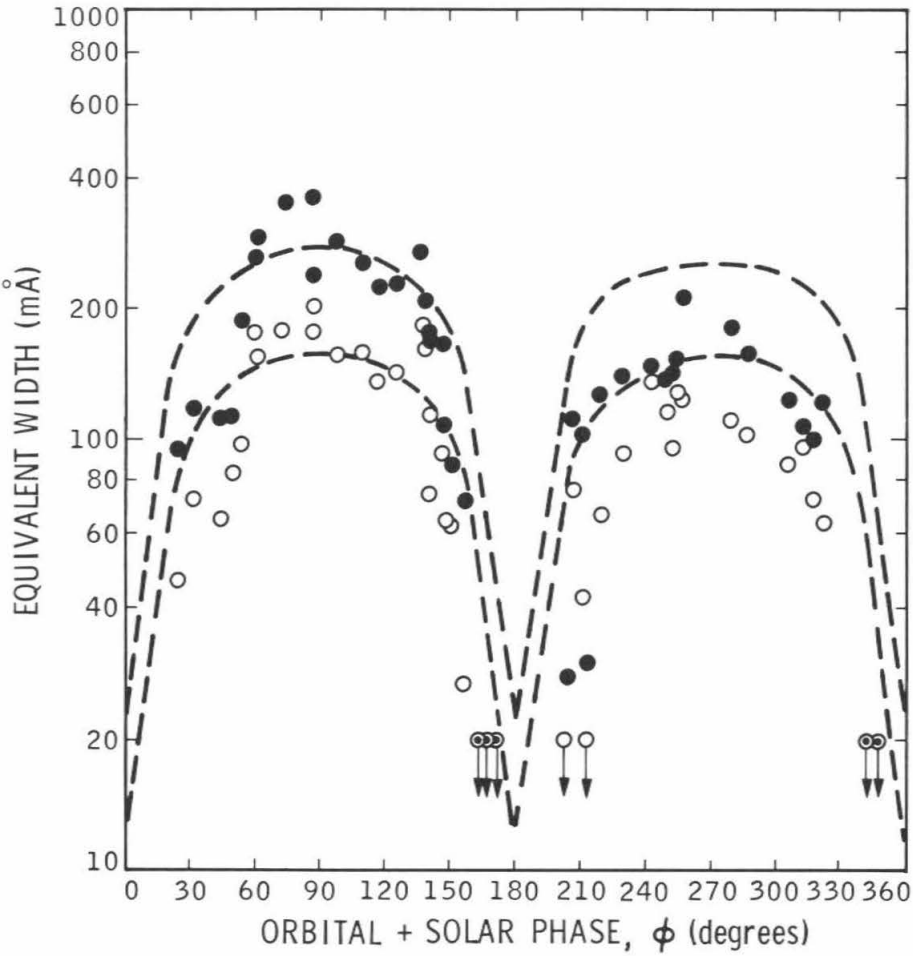

Fig. 8. The D_2 (filled circles) and D_1 (open circles) emission line equivalent widths observed by Bergstralh *et al.* (1975). The data are plotted versus orbital plus solar phase angle, which is θ_{SHC}, the angle from superior heliocentric conjunction. The dashed curves are the solar excitation values scaled to match the 90° emission peak for both D_2 and D_1.

tures. Nevertheless, from the conclusion drawn in D above, the emission lines probably originate in Region *B*, but the light has been mixed into Region *A* observationally by blurring effects collectively called "seeing."

A simple measurement of the recorded line width does not translate directly into a kinetic temperature for the sodium. Several effects contributing to the linewidth must be accounted for: instrumental broadening, radiative transfer effects, variation of Doppler shifts and intensities during the observation, and hyperfine structure of sodium. Removing these effects, Brown *et al.* (1975), using a single-component model, report a residual

breadth which translates to a sodium kinetic temperature of 5200 ± 2300°K. Macy and Trafton (1975) have interpreted their similar linewidth measurement to imply a much lower temperature, 500–1000°K, on the basis of a two-component scheme. They envision an optically very thick kernel close around Io in addition to an optically thin contribution from Region *B*. The broad line from the cooler source results from the large radiative transfer correction associated with the thick component.

Bulk motion is a potential source of systematic error in determinations of the sodium temperature from Doppler-shift measurements as mentioned in Sec. I.C.

The few observations of the sodium emission in Region *B* which have combined photometric calibration with good spatial resolution are consistent with a partial torus of sodium leading and trailing Io in its orbit. This elongated cloud is optically thin to within a few arcsec from Io, where it reaches at least unit optical depth. The published observations are, first, spectra taken at localized points near Io, such as shown in Fig. 7 and otherwise described in Trafton *et al.* (1974), Trafton and Macy (1975) and Macy and Trafton (1975). Second, Brown *et al.* (1975) have reported a one dimensional profile of Region *B* parallel to the orbital plane within about 10 arcsec of Io. This is shown in Fig. 9.

Preliminary two-dimensional images described by Münch and Bergstralh (1975) are also consistent with the partial torus geometry. The uncalibrated long-slit spectra revealing Region *C* show that the torus may be complete at low emission levels; these data are discussed below.

A recorded apparent emission rate can be translated into a column abundance along the line of sight on the basis of Eq. (18). However the g-value must be known in order to do this with accuracy, and that requires knowing what velocity characterizes the bulk motion of that portion of the cloud. Brown *et al.* (1975) assumed, in the absence of better information, that the value of g for the optically-connected cloud was the same as for Io. Sodium distributed along Io's orbit must surely have a range of sodium-Sun Doppler shifts and therefore experience a range of g-values. The only published observations pertinent to this topic are the 22 October 1973 spectra of Trafton *et al.* (1974) and a Region *C* spectrum of Mekler and Eviatar (1974). The latter is discussed below. The former reports the same sodium-Earth Doppler shift for rather widely separated spots in Region *B*. Trafton and Macy (1975) have recently reported asymmetrical D-line profiles in spectra taken at very high resolution which may point to differential bulk motion in the Region *B* sodium cloud on the scale of a few arcsec.

The question of the D_2/D_1 ratio in Region *B* differing from the value ($D_2/D_1 \approx 1.8$) expected for a solar resonant scattering mechanism has been rather widely discussed in the literature. There are simply not enough high-quality measurements of that ratio to indicate that there is a problem.

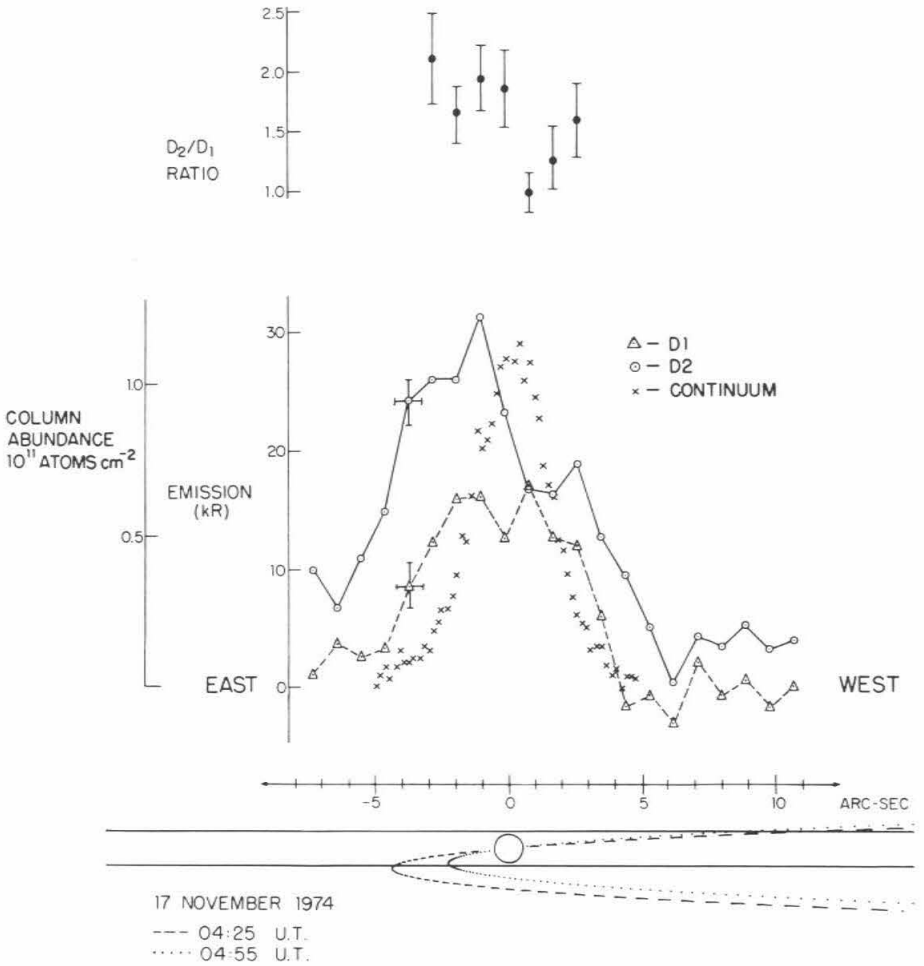

Fig. 9. A one-dimensional profile of the Region *B* sodium emission. At bottom, the geometric disc of Io is shown fixed in the projected slit. The orbit, which drifted with respect to the slit, is sketched for the beginning and end of the observation. At center, the D_1 and D_2 emission profiles are plotted on the same abscissa. Each point is both an average over one arcsecond of height along the spectrograph slit and an integration over 0.64 Å along the dispersion. The continuum profile locates Io's image and is scaled arbitrarily. The sodium column abundance scale is valid for the D_2 emission. At the top, the D_2/D_1 ratio is plotted over the range in which it is well determined. (From Brown *et al.* 1975).

F. Sodium in Region C

Detection of D-line emission remote from Io has been reported by Mekler and Eviatar (1974), Wehinger and Wyckoff (1974), Mekler *et al.* (1975) and Wehinger *et al.* (1976). All these observations were made with the same

instrument, namely the fast and efficient low-dispersion image tube spectrograph at the Wise Observatory of Tel-Aviv University. Little quantitative work has been reported, but visual inspections of the plates have led the investigators to describe a highly flattened distribution of sodium emission concentrated in the orbital plane of the satellites. In that plane it is discernable to about 4 (Mekler *et al.* 1975) or 10 (Wehinger and Wyckoff 1974) arcmin from Jupiter. It is visible $\frac{1}{2}$ to 1 arcmin above and below the orbital plane, and even over the poles of Jupiter (Wehinger *et al.* 1976). Mekler *et al.* (1975) refer to an inner limit to the distribution about 1 arcmin from Jupiter.

To dramatize the extent of Region *C*, we note that the elongations of Io's orbit are a little more than 2 arcmin from Jupiter. During the past two years the jovicentric declination of the earth has been less than about 1°.7, which means that the semi-minor axis of Io's apparent orbit was less than about 4 arcsec for the period of these observations.

Wehinger *et al.* (1976) report photometric comparison of their Region *C* observations with the 5577 Å telluric airglow line due to atomic oxygen. They find D-line intensities between 100 R and 2 kR in the orbital plane.

Mekler and Eviatar (1974) report that on one occasion they observed a strong tilt of the D emission line with respect to the telluric airglow lines on the same spectrum. The sodium line extended about 2 arcmin along the projected slit, which was oriented at 25° with respect to the orbital plane. The Doppler-shift difference between the two ends of the emission line translates to a velocity difference of 200 km sec^{-1}. Wehinger *et al.* (1976) report that they have not observed this tilting effect.

The photometric reduction of image tube spectra of the Region *C* emission must be done with great care. Visual inspection of the Mekler *et al.*, (1975) spectra show strong contamination by non-linear response in the photographic emulsion. The emission lines are superimposed on Jupiter's or a satellite's scattered continuum which varies over the height of the slit and biases the response to the emission lines to different parts of the film's characteristic curve. The result is seen as non-uniformity over the height of the slit of the 5577 Å airglow line. It is not clear to what extent this effect has influenced the qualitative conclusions drawn by the observers from these plates.

II. ULTRAVIOLET EMISSION OBSERVED FROM PIONEER 10

The "H" channel of the two-color ultraviolet photometer aboard Pioneer 10 recorded emission originating in the vicinity of Io. These measurements have been described by Judge and Carlson (1974) and Carlson and Judge (1974, 1975).[3] We summarize here the rather sparse observational knowledge

[3]See p. 1079.

about the source, its spatial distribution and the mechanism which excites the ultraviolet emission.

The investigators tentatively identified the emission as Lyman α resonantly scattered by atomic hydrogen. The transition has a large oscillator strength, the solar flux is high at that wavelength (1216 Å), and hydrogen is an abundant element. However, the identification cannot be considered definitive. Figure 10 shows the spectral responses of the two channels. The fact that the emission was seen only in the "H" channel simply constrains the wavelength to be greater than 800 Å. However, increasingly higher emission rates are required than those derived on the basis of the Lyman α identification if the actual wavelength is longer than 1216 Å.

The ultraviolet emission comes from an elongated section of Io's orbit approximately centered on the satellite. This is shown in Fig. 11, which is from Carlson and Judge (1975).

An upper limit to the extent of the emission normal to Io's orbital plane was established by the emission's disappearance in solar eclipse by Jupiter: it is less than one Jupiter diameter thick. This observation also implies that the excitation mechanism is solar resonance scattering.

If the emission is Lyman α, the apparent emission rate of the hydrogen cloud is $\sim$ 300 R. The radial column abundance is calculated to be $\sim 3 \times 10^{12}$ cm^{-2}, which corresponds approximately to unit optical thickness in Lyman α. The implied total population of the cloud is $\sim 2 \times 10^{33}$ atoms (Carlson and Judge 1974).

III. OTHER OPTICAL LINE EMISSIONS

No optical emissions from Io or its vicinity have yet been positively identified other than those discussed in Secs. I and II, though there have been intensive but not exhaustive searches.

Mekler and Eviatar (1974) reported the possible detection of emission by neutral calcium at 4227 Å. Using the Wise Observatory's image tube spectrograph, a continuum spectrum of Io (Io in the spectrograph slit) and a spectrum of the moon were taken. They compared the central intensities of two Fraunhofer lines at 4227 Å (CaI) and 4236 Å (FeI), and found the calcium feature for Io to be 10% less deep than for the moon. Assuming the iron line to be constant, the observers ascribed this difference to calcium emission from Io's Region *A*. This procedure is doubtful due to the substantially different strengths of the two Fraunhofer features which were compared. Two possible sources of systematic error not considered by Mekler and Eviatar are the consequences of non-linear detection and the ring effect, most recently discussed by Barmore (1975).

The same calcium resonance line has been sought by other observers using higher-precision techniques, but it has not been detected (Macy and

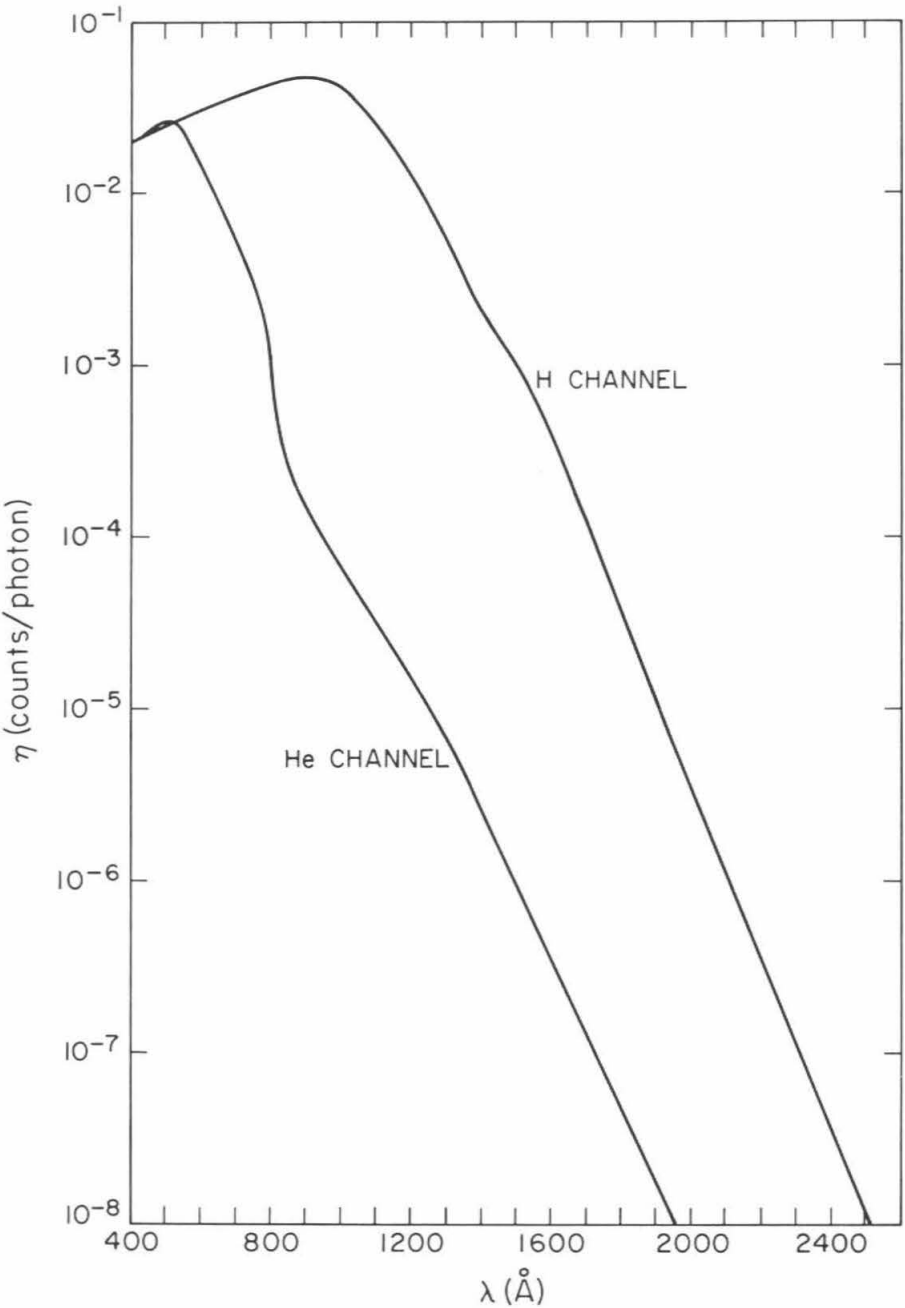

Fig. 10. Spectral response of the UV ultraviolet photometer on Pioneer 10. The quantum efficiency in photoelectrons per photon is shown for the two channels as a function of wavelength and includes photoelectric response, filter transmission and collection efficiency. (From Carlson and Judge 1974.)

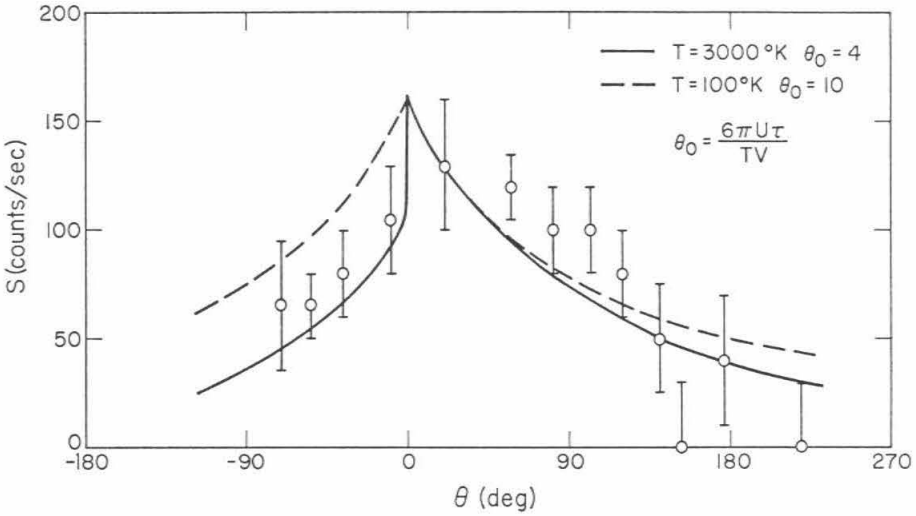

Fig. 11. The observed H Lyman-α intensity as a function of the orbital angle with respect to Io. Positive values of θ are for the trailing portion of the cloud. The figure is taken from Carlson and Judge (1975), and the curves are for their models of the hydrogen cloud formation.

Trafton 1975; Brown *et al.* 1975). The upper limits to 4227 Å emission quoted by these authors is about 5 kR referred to the size of Io's disc.

A possible detection of helium emission from Io at 10,830 Å was reported by Cruikshank *et al.* (1974). They have since announced that the observation was spurious and due to an instrumental problem that is now understood. Macy and Trafton (1975) have reported that 0.5 kR of 10,830 Å emission from the spatially uniform telluric airglow was observed when they attempted confirmation of the earlier report.

Other negative results have been reported. From Trafton *et al.* (1974) with no quoted upper limit: 6160.7 Å (NaI), 8194.8 Å (NaI), 6707.8 Å (LiI), 7699.0 Å (KI), 5183.7 Å (MgI) and 6300.2 Å (OI). Macy and Trafton (1975) report the following upper limits: 5 kR of 6707.8 Å (LiI), 5 kR of 7699.0 Å (KI) and 0.17 kR of 4571 Å (MgI). These measurements were made with Io in the spectrograph slit.

Recently Trafton (1976) has reported observations of Region *B* in the spectral range 3100 Å to 8700 Å. No emission feature other than the D-lines was found. Upper limits are 0.4 – 0.6 kR in the red, 0.6 – 1.6 kR in the green and blue, and up to 5 kR in the violet.

The Region *C* spectra of Wehinger *et al.* (1976) were examined for emission features other than the sodium D-lines and telluric airglow lines. The detection limit at 5900 Å was below 100 R. No new features were discovered between 3500 Å and 9000 Å.

IV. FUTURE OBSERVATIONAL WORK ON IO'S LINE EMISSIONS

Observations during the 1975–76 apparition of Jupiter will probably result in a clearer description of the spatial distribution and motions of Io's sodium cloud. Io's orbital period is about 42 hours and we view its orbit from the side, so a series of two-dimensional D-line images are required to visualize the cloud's morphology. The instrumental difficulties inherent in this task are formidable. Jupiter and a halo of its light scattered in the optics dominate the field of view, and in the immediate vicinity of Io the skirts of Io's seeing disc also contribute a continuum background. To achieve good contrast between the narrow emission lines and this background, conventional techniques require high spectral resolution. Continuing an example given in Sec. I.B, consider Io with opposition magnitude and 2 arcsec seeing. Suppose we wish to image a portion of Region *B* where the continuum apparent emission rate of Io is down from its central value by a factor $q = E/E_0$ while $E_0 = 1.5$ MR Å^{-1}. Using a filter with bandpass $\Delta\lambda$ the ratio of D-line to continuum signal is

$$\frac{S}{N} = \frac{E_D}{\Delta\lambda\, q\, E_0}. \tag{22}$$

Taking $q \simeq 10^{-2}$ and $E_D = 10$ kR, the requirement on the spectral resolution for $S/N = 10$ is

$$\Delta\lambda \lesssim 0.1 \text{ Å} \tag{23}$$

which is rather severe.

Imaging techniques at high spectral resolution will provide important information about the sodium's motion by measuring the Doppler shift. An innovative imaging technique is being developed by Mertz (1975) for studying Io's sodium cloud. With an interferometer he creates fringes across the telescopic field in D-line radiation; the background continuum radiation produces no fringes. The distribution of sodium is present as AC information on the detector and is recovered by a heterodyne technique. A similar technique has been described by Blamont and Courtès (1955).

The search for other optical emissions from Io's environment will be continued. To discover such emissions from Region *B*, near Io, is an easier observational task than looking for features on the continuum spectrum of Io. This point follows from the discussion in Sec. I.D of contrast with Io's continuum radiation. Io's albedo rises steeply from the ultraviolet to near infrared, with Lambert-sphere-equivalence achieved near 0.6 μm. The Region *A* contribution of an isotropic resonant scatterer is in the sense of an emission line for shorter wavelengths and an absorption feature for longer wavelengths, but the contrast is low. However, if the constituent is also in Region *B*, then its resonance line may have good observational contrast against the dark sky for spectra taken with Io just outside the spectrograph slit.

V. IO'S IONOSPHERE

The only existing evidence of an atmosphere on Io is the two electron density profiles in Fig. 12, deduced by Kliore *et al.* (1975) from the S-band occultation experiment on Pioneer 10. The electron density distribution on the dayside shows a peak concentration of 6×10^4 cm^{-3} at an altitude of 100 km and an extent of 750 km with a nearly constant scale height of 200 km. On the nightside the peak electron density is 1×10^4 cm^{-3} and the ionosphere appears to cut off abruptly above 200 km. These peak electron densities are comparable to those observed on Mars and Venus (Kliore *et al.* 1965; Kliore *et al.* 1967), even though the solar flux at Io is much weaker. This sets important constraints on the rates of production and loss of ions. The contrast between the day and night profiles suggests that ions are removed in a time shorter than an Io day (42 hours).

In this section we review four existing models for Io's ionosphere. The basic assumptions and predictions of each are summarized in Table III. As a group they can be criticized for being parochial; they are based on our experience with the atmospheres of the terrestrial planets and ignore, or do not fully account for, the interaction between Io and the Jovian magnetosphere. Detailed plasma interaction models are currently being studied by F. M. Neubauer,[4] Shawhan (1975) and the Harvard group under McElroy. We conclude this section with a summary of what we have learned from studying the ionosphere of Io.

A. *The Webster* et al. *Model*

The Webster *et al.* model (1972) was motivated by the decametric radiation theory of Goldreich and Lynden-Bell (1969). Proposed before the Pioneer 10 encounter, it is inadequate in a number of ways, but it conveys the spirit of later photochemical models. The bulk atmosphere is assumed to consist largely of methane with a surface number density of 10^{13} molecules cm^{-3}. The primary process of interest is photoionization of CH_4 by ultraviolet sunlight:

$$CH_4 + h\nu \rightarrow CH_4^+ + e \tag{24}$$

followed by dissociative recombination

$$CH_4^+ + e \rightarrow CH_3 + H\,. \tag{25}$$

The electron number density $[n_e]$ is simply given by

$$[n_e] = \{J[CH_4]/\alpha\}^{\frac{1}{2}} \tag{26}$$

where $[CH_4]$, J and α respectively denote CH_4 number density (cm^{-3}), photoionization rate (sec^{-1}) and dissociative recombination coefficient (cm^3

[4]Oral presentation at the Io Week Workshop, Feb. 22, 1975, Harvard University.

TABLE III

Summary of Io Model Ionospheres

ASSUMPTIONS	Webster *et al.*	McElroy & Yung (*A*)	McElroy & Yung (*B*)	Whitten *et al.*
Atmospheric Composition (cm^{-3})	CH_4 (1×10^{13})	NH_3, N_2, Na (10^{11})[a], (10^9), (3×10^6)	NH_3 (10^{11})	Ne (4×10^9)
Atmospheric Temperature	100°K	500°K	500°K	160°K
Major Ion	CH_4^+	Na^+	NH_3^+	Ne^+
Electron Source	$CH_4 + h\nu \rightarrow CH_4^+ + e$	$Na + h\nu \rightarrow Na^+ + e$	$NH_3 + p \rightarrow NH_3^+ + p + e$ $NH_3 + e \rightarrow NH_3^+ + e + e$	$Ne + h\nu \rightarrow Ne^+ + e$
Electron Loss	$CH_4^+ + e \rightarrow CH_3 + H$	$Na^+ + e \rightarrow Na + h\nu$ Diffusion to surface	$NH_3^+ + e \rightarrow NH_2 + H$	Diffusion to surface
PREDICTIONS				
Peak Electron Density	7×10^3 cm^{-3}	6×10^4 cm^{-3}	6×10^4 cm^{-3}	1×10^5 cm^{-3}
Altitude of Peak	200 km	100 km	100 km	50 km
Scale Height	58 km	200 km	200 km	200 km
Time Constant	10^3 sec[b]	one Io day	not estimated	one Io day

[a]at night $[NH_3] = 10^9$ cm^{-3} [b]estimated by present authors

sec^{-1}). The model successfully predicts the existence of an ionosphere. The computed $[n_e]$ profile is illustrated in Fig. 13. By varying the surface number density of CH_4 and the atmospheric temperature[5] as parameters we can adjust the model to agree with the Pioneer 10 observations in many essential aspects. But the small peak electron density is an intrinsic feature of this model, indeed of any other model in which the dominant ion is a molecular ion produced by photoionization and removed by dissociative recombination (cf. Model 1 of McElroy and Yung 1975).

It is interesting to note that the first model of an atmosphere on Io suggests that Io would be a large source of hydrogen. Photolysis of CH_4 by sunlight readily leads to production and escape of hydrogen at a rate $\sim 10^{10}$ atoms cm^{-2} sec^{-1}:

$$CH_4 + h\nu \rightarrow CH_3 + H\,. \tag{27}$$

Webster *et al.* did not pursue the consequences of methane dissociation.

B. The McElroy and Yung Model (A)

The column abundance of sodium atoms in Region *B* has been observed to be $\sim 10^{11}$ cm^{-2} (Brown *et al.* 1975). The amount of sodium in Region *A* cannot be estimated directly from observations for reasons discussed in Sec. I.D. But, if Io is the source of sodium atoms in the cloud, the atmosphere probably contains more than 10^{12} sodium atoms cm^{-2}.

The possibility of an ionosphere with Na^+ as the major ion was first recognized by McElroy *et al.* (1974) prior to the Pioneer 10 encounter. The idea was pursued and developed by McElroy and Yung (1975). They proposed an ammonia atmosphere with sodium as a minor component. Because of its low ionization potential (5.14 eV), sodium atoms are readily ionized by absorption of ultraviolet photons shortward of 2412 Å:

$$Na + h\nu \rightarrow Na^+ + e\,. \tag{28}$$

The Na^+ ions will be removed via radiative recombination:

$$Na^+ + e \rightarrow Na + h\nu \tag{29}$$

and by molecular diffusion to the surface. Note the crucial difference between an atomic ion like Na^+ and a molecular ion like CH_4; the radiative recombination coefficient for an atomic ion is typically about 10^5 times slower than the dissociative recombination coefficient for a molecular ion. Consequently the presence of even a small concentration of sodium atoms in the atmosphere could lead to the formation of large numbers of sodium ions. The model includes details of molecular diffusion, diurnal variation, and bulk vertical motion due to condensation and evaporation of ammonia. The results for electron number densities are illustrated in Fig. 14.

---

[5]In an internally consistent model, the temperature must be calculated from the heating rate based on atmospheric composition and is not a free parameter.

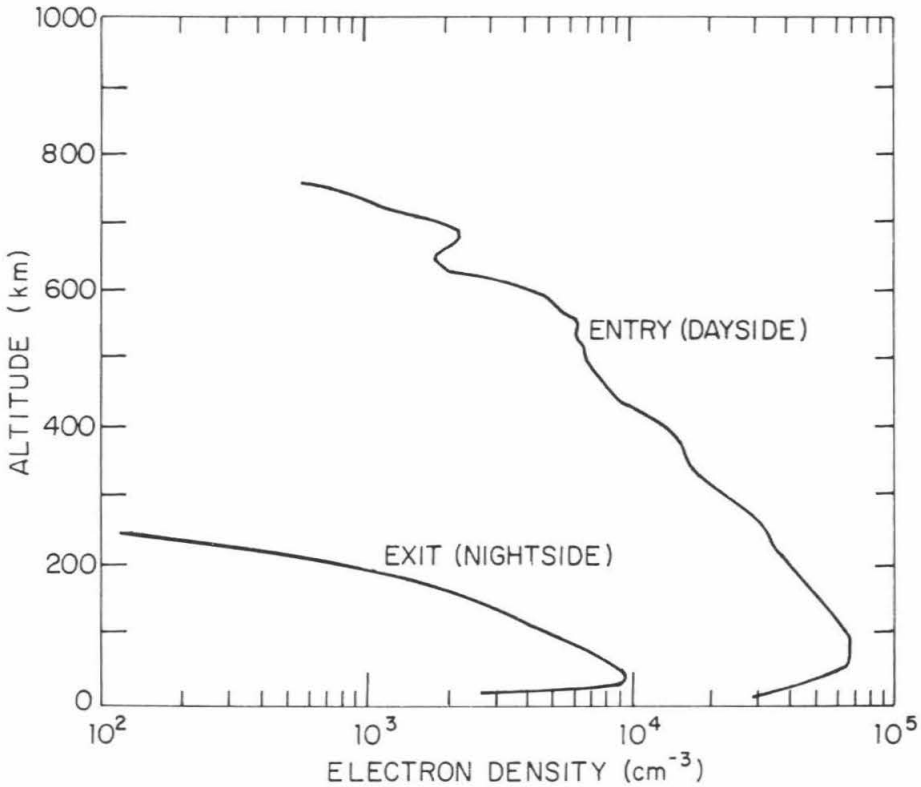

Fig. 12. Entry (dayside) and exit (nightside) electron density profiles as measured on Io by Pioneer 10. (Kliore *et al.* 1975.)

C. The McElroy and Yung Model (B)

A model involving charged energetic particles in the Jovian radiation belt as the ionization source was explored by McElroy and Yung (1975). The major atmospheric gas is assumed to be NH_3. NH_3^+ ions are primarily produced by proton or electron impact:

$$\begin{aligned} NH_3 + p &\rightarrow NH_3^+ + e + p \\ NH_3 + e &\rightarrow NH_e^+ + e + e\,. \end{aligned} \tag{30}$$

The loss mechanism is dissociative recombination:

$$NH_3^+ + e \rightarrow NH_2 + H\,. \tag{31}$$

The cross-section of a 10 Mev proton or a 10 kev electron is about 10^{-18} cm^2 and varies as $\log E/E$, where E is the energy. The calculation shows that it is possible to account for the principal features of the observed ionosphere

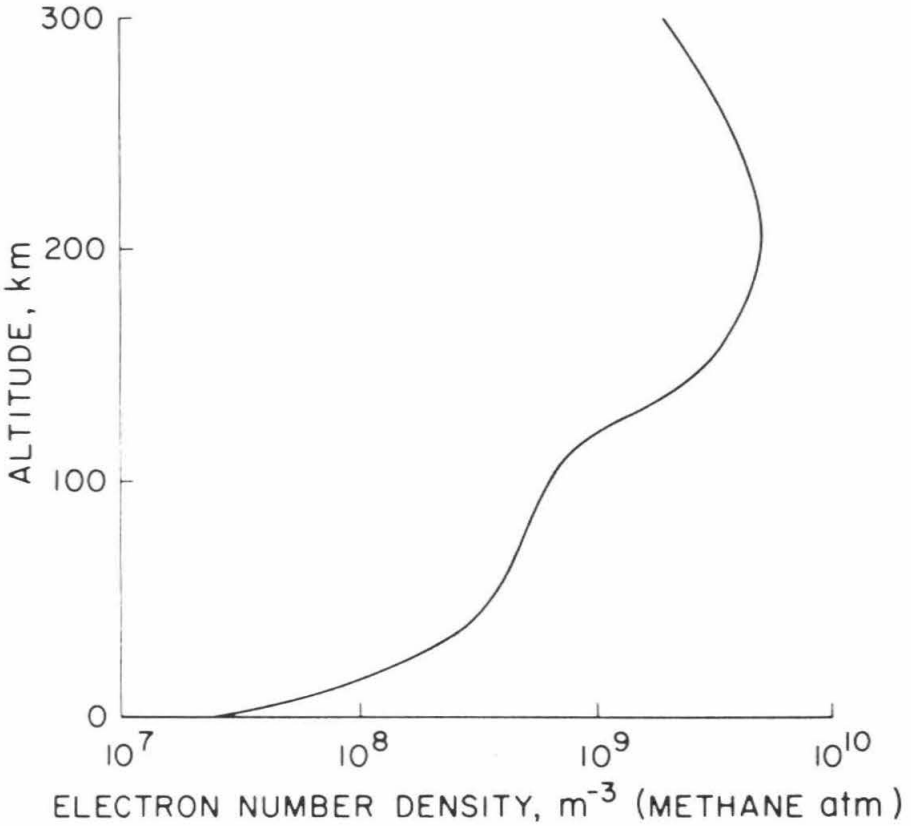

Fig. 13. Electron number density as a function of altitude at the subsolar point in the methane atmosphere assumed for Io. (Webster *et al.* 1972.)

with a flux of 3×10^7 cm^{-2} sec^{-1} of 10 Mev protons impinging on an atmosphere with a surface number density equal to 3×10^{11} cm^{-3}. The results are shown in Fig. 15. To explain the diurnal difference, it must be postulated that the energetic particles are entering Io's atmosphere asymmetrically, a view consistent with the implications of the electromagnetic interactions in the vicinity of Io (Shawhan *et al.* 1974; Shawhan 1976).

D. The Whitten et al. *Model*

Recently Whitten *et al.* (1975) proposed a neon ionosphere. Io is assumed to have a tenuous neutral atmosphere composed of neon with surface density about 4×10^9 cm^{-3}. Photoionization is the main source of Ne^+. Loss of ions is due to diffusion to the surface. The main feature of the model, as the authors pointed out, is that the neutral atmosphere is relatively cold ($\sim$ 160°K) and tenuous. The neon model does not treat Io's hydrogen source,

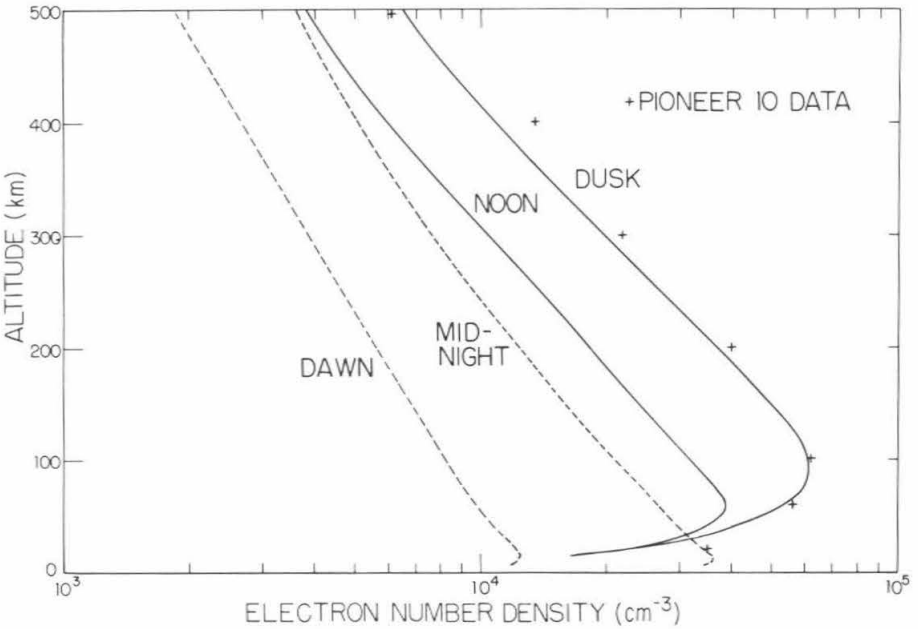

Fig. 14. Electron density profiles for Io's ionosphere. Na^+ is the major ion. NH_3 is the major neutral species. In the daytime the surface number density of Na and NH_3 is taken to be 3.7×10^6 cm^{-3} and 5.0×10^{10} cm^{-3} respectively. At night NH_3 is reduced by a factor of 5 and a vertical downward motion of 5 m sec^{-1} is imposed on the atmosphere. The calculation is carried out for an isothermal atmosphere at 500°K. (McElroy and Yung 1975).

and it ignores a potentially important reaction with sodium. Charge transfer by neon ions to sodium atoms is probably fast,

$$Ne^+ + Na \rightarrow Ne + Na^+ . \tag{32}$$

The chemical lifetime for Ne^+ is given by

$$\tau = \frac{1}{k \cdot [Na]} \tag{33}$$

where k is the charge-transfer rate coefficient and [Na] is the number density of sodium atoms. If we assume $k \approx 10^{-9}$ cm^3 sec^{-1} and [Na] $\approx 10^5$ cm^{-3}, then $\tau \approx 10^4$ sec, a value which is comparable to the diffusion time constant and suggests that Na^+ probably cannot be ignored. This reaction may be important.

E. Tentative Conclusions about Io's Neutral Atmosphere

From the study of a variety of models of Io's ionosphere, we are able to suggest tentative answers to two important questions about Io's neutral at-

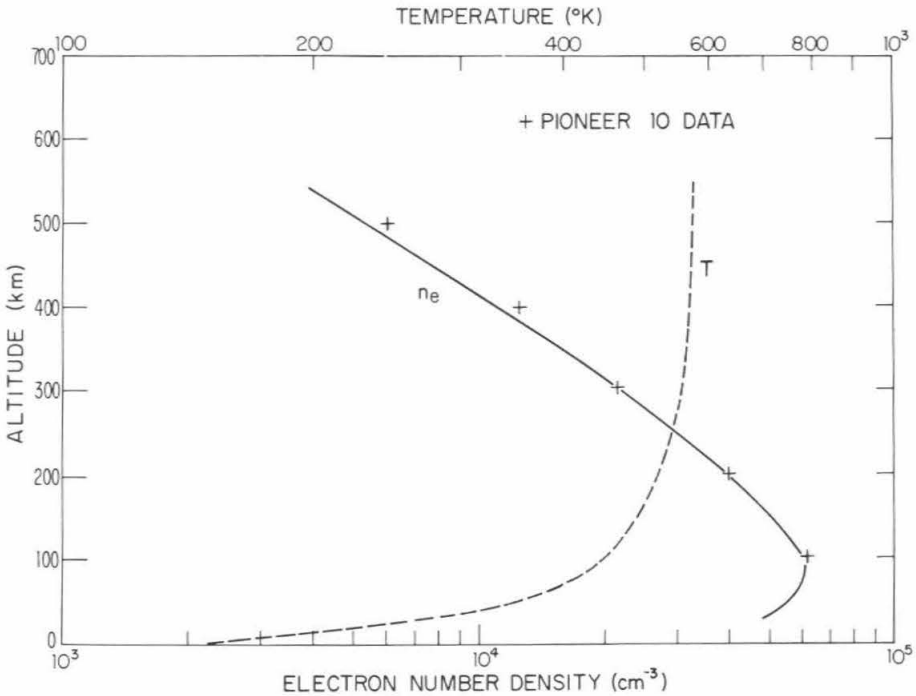

Fig. 15. Electron number density and atmospheric temperature profiles computed with the McElroy and Yung Model *B*. (McElroy and Yung 1975.)

mosphere: how hot was it at the time of the encounter and how dense is it?

For ambipolar diffusive equilibrium, the plasma scale height is given by

$$H = \frac{k}{m_0 g}\left[\frac{T_e + T_i}{A_i}\right] \tag{34}$$

where m_0 is the atomic mass unit, k is the Boltzmann constant, g is Io's gravitational acceleration, A_i is the mass number of ion species, and T_e and T_i are the electron and ion temperatures respectively (cf. Bauer 1973). Assuming $T_e = T_i$ and using $g = 178$ cm sec^{-2} (Anderson *et al.* 1974), the scale height observation implies

$$\frac{T_i}{A_i} = 21.5\,. \tag{35}$$

We must emphasize that the expression is derived on the assumption of diffusive equilibrium for the ions. Inclusion of a solar-wind type interaction can seriously modify the interpretation (Cloutier *et al.* 1969). For protons the implied temperature is 21.5°K, for Na^+ it is 500°K. In thermodynamic equi-

librium, T_i equals T_n (the temperature of the neutral atmosphere), but in general T_i is higher than T_n. The inequality

$$T_n < T_i = 21.5\, A_i \tag{36}$$

implies, for reasonable values of A_i, that the neutral atmosphere did not exceed 1000°K at the time of Pioneer 10 encounter.

The inference of a lower limit to the density of the neutral atmosphere from the detected ionosphere is model-dependent. In the Whitten *et al.* Model, the absolute lower limit is $\sim 4 \times 10^9$ cm^{-3}. Below this value loss of ions by diffusion will be too fast and the computed ionospheric peak will be too small to account for the observations.

In the McElroy and Yung Model *A*, the constraint of the ionosphere is

$$N_0 \cdot [\mathrm{Na}]_0 \approx 10^{16}\ \mathrm{cm}^{-6} \tag{37}$$

where N_0 is the neutral number density and $[\mathrm{Na}]_0$ is the sodium number density at the surface. The flux of neutral Na atoms to the surface is given by

$$\phi = -D\left\{\frac{\mathrm{d}[\mathrm{Na}]}{\mathrm{d}z} + \frac{[\mathrm{Na}]}{H}\right\} \approx -D\,\frac{[\mathrm{Na}]_0}{H}\ \mathrm{cm}^{-2}\ \mathrm{sec}^{-1} \tag{38}$$

where D is the diffusion coefficient and H is the scale height. Combining Eqs. (37) and (38),

$$\phi \times N_0^2 \approx 3 \times 10^{27}\ \mathrm{cm}^{-8}\ \mathrm{sec}^{-1}\,. \tag{39}$$

Thus, if we require $\phi < 10^7$ cm^{-2} sec^{-1}, then $N_0 \gtrsim 1.7 \times 10^{10}$ cm^{-3}.

In McElroy and Yung Model *B* the relationship between N_0 and the flux of energetic particles f_0 is given by

$$N_0 f_0 \approx 3 \times 10^{18}\ \mathrm{cm}^{-5}\ \mathrm{sec}^{-1}\,. \tag{40}$$

The Pioneer 10 measurements impose an upper limit of about 10^9 cm^{-2} on f_0, and hence $N_0 > 3 \times 10^9$ cm^{-3} for this model.

Since McElroy and Yung Models *A* and *B* only when combined touch on all the observational aspects—the sodium and hydrogen as well as the ionosphere—we consider that a best estimate to the neutral density is

$$N_0 \approx 10^{10}\ \mathrm{cm}^{-3} \tag{41}$$

a value which is about two orders of magnitude lower than the upper limit deduced from the observations of the β-Scorpii occultation (Taylor *et al.* 1971; Smith and Smith 1972).

VI. IO AS A SOURCE OF HYDROGEN

As discussed in Sec. II, the Pioneer 10 ultraviolet observations suggest that Io is surrounded by an extensive hydrogen cloud containing $\sim 10^{33}$ hydrogen atoms. To account for the cloud's geometry Carlson and Judge

(1974) and McElroy and Yung (1975) independently estimated a lifetime of $\sim 10^5$ sec for the hydrogen atom. This lifetime is considerably shorter than the photoionization lifetime of $\sim 10^8$ sec and is probably due to charge transfer of hydrogen atoms with low-energy protons in the Jovian magnetosphere. The calculations suggest the existence of a low-energy proton flux $\sim 10^9$ cm^{-2} sec^{-1}, a result that has recently been supported by the detailed analysis of plasma observations by Pioneer 10 in the neighborhood of Io's flux tube (Frank *et al.* 1975). If Io were the only source of hydrogen, a mean flux of $\sim 10^{11}$ atoms cm^{-2} sec^{-1} must be supplied from the surface of Io to maintain the observed cloud in the steady state. But we have no observational evidence that the hydrogen cloud is in a steady state, so the actual demand on the hydrogen source could be much lower. We will next consider the implications for the hydrogen source in three subsections. In A we examine photolysis of NH_3 as a source of H, and in B we discuss the possibility of cycling hydrogen with magnetospheric protons. In C possible escape mechanisms for hydrogen are discussed.

A. Photolysis of NH_3 as the Source of Hydrogen

If the hydrogen cloud were assumed to be in a steady state with the supply coming solely from Io, the required flux would be 10^{11} atoms cm^{-2} sec^{-1} at Io's surface. Such a large escape rate can best be appreciated by noting that it would represent loss of over 10 km of surface material to space in the age of the solar system. It is reasonable to hypothesize that the surface of Io contains a volatile material rich in hydrogen. Evaporation of this material and its subsequent photolysis can provide a large source of atomic hydrogen. Ammonia frost is an obvious candidate, but arguing against its presence is the lack of ammonia absorption features in the infrared spectrum of Io (Fink *et al.* 1973; Pilcher *et al.* 1972). McElroy *et al.* (1974) have thoroughly discussed the various aspects of the ammonia hypothesis. The most important reason for assuming an ammonia atmosphere is the need to supply a huge escape rate of hydrogen. The most serious problem associated with this model is the escape of nitrogen, the terminal product of photodissociation of ammonia. Note that the nature of the problem is not changed if we assume a methane atmosphere. Photolysis of a hydrogen-bearing molecule releases the hydrogen atoms and leaves the heavy "residue" in the atmosphere. The rate at which the heavy component would accumulate must essentially equal the rate of hydrogen escape and would result in an atmosphere in excess of the observed upper limit in less than 10 years. To circumvent the problem of a rapid build-up of the end-products of photolysis, McElroy *et al.* (1974) postulated escape of a large amount of gases during periods of intense heating in the upper atmosphere initiated by the precipitation of energetic particles from the radiation belt.

B. *Proton Exchange*

Fanale *et al.* (1975, 1976) have made the most complete study of the surface of Io based on its photometric properties, and they also considered cosmochemical composition and thermal history. They concluded that Io's properties could best be explained by postulating that it is largely covered by evaporite salts, rich in sodium and sulphur. They considered the presence of large amounts of frost unlikely. In view of this model it is reasonable to ask whether there is an alternative to ammonia ice as a source for the hydrogen cloud observed by Pioneer 10.

Protons in the extensive magnetosphere of Jupiter obviously represent a potential hydrogen source. Frank *et al.* (1975) have analyzed the directional, differential spectrum for proton densities $\frac{\partial J}{\partial E}$ (cm^2-sec-ster-eV)$^{-1}$ at positions inside the Io flux tubes. The proton spectrum is approximated well by a Maxwellian distribution with proton number density $N_p = 60$ cm^{-3} and mean energy $\epsilon_p = 95$ eV. The flux of protons impinging on Io is on the order of

$$N_p \sqrt{\frac{2\epsilon_p}{M_p}} \approx 10^9 \text{ cm}^{-2} \text{ sec}^{-1} \tag{42}$$

where M_p is the proton mass.

This falls about two orders of magnitude short of the required source, so a large number of protons outside the observed energy range must be postulated to make this a viable mechanism. McDonough (1975) proposed an interaction between Io and a low-energy component of the magnetospheric plasma. The latter is assumed to originate from Jupiter and could provide a source of hydrogen atoms to Io. But again it is not clear that this mechanism can provide enough hydrogen to explain the observations.

In view of the uncertainties of observations and models we do not regard this deficiency as serious, especially since we have no observational evidence for the stability of the hydrogen cloud. The magnetospheric protons could be thermalized and accumulated in the atmosphere and blown off sporadically when the atmosphere is heated by an electromagnetic interaction.

C. *Hydrogen Escape*

Escape of a light species like hydrogen from Io is an efficient process. A hydrogen atom with the thermal kinetic energy associated with temperatures in excess of 190°K can escape Io's gravity. The escape rate is given by the Jeans formula

$$\phi = \frac{n_c v_o}{2(\pi)^{\frac{1}{2}}} (1 + \lambda) e^{-\lambda} \tag{43}$$

where n_c is the hydrogen number density at the exobase, $v_o = (2kT/m)^{\frac{1}{2}}$ and $\lambda = GM_I/rkT$ (Chamberlain 1965). All the current models on the dynamics

of the hydrogen cloud (Carlson and Judge 1974; Smyth personal communication 1975) are based on Jeans' theory, modified somewhat to include effects of the three-body gravitational interaction and the possibility of non-thermal velocity distribution for the escaping atoms. A crucial assumption in deriving the Jeans result is that the atmosphere is in hydrostatic equilibrium:

$$\frac{\mathrm{d}}{\mathrm{d}r}(nkT) + \frac{GM_I mn}{r^2} = 0 \tag{44}$$

where n = number density of gas, and other symbols have their usual meanings. Parker (1958) has shown that for thermal energy large compared with gravitational energy the hydrostatic equation must be replaced by a set of hydrodynamic equations

$$mnv\frac{\mathrm{d}v}{\mathrm{d}r} + \frac{\mathrm{d}}{\mathrm{d}r}(nkT) + \frac{GM_I mn}{r^2} = 0 \tag{45}$$

$$\frac{\mathrm{d}}{\mathrm{d}r}(r^2 nv) = 0\,. \tag{46}$$

Physically, Eq. (45) is the equation of motion obtained by adding an inertial term to Eq. (44), and Eq. (46) therefore is the equation of continuity. When the thermal energy per particle exceeds its gravitational potential energy, that is,

$$\frac{3}{2}kT > \frac{GM_I m}{r} \tag{47}$$

the gas is free to expand rapidly or "blow-off" (Öpik 1963). For Io the critical temperature for the stability of a hydrogen-dominated exosphere is 216°K (Gross 1974), so from our understanding of the ionosphere the temperature in Io's upper atmosphere probably exceeds the blow-off temperature for hydrogen.

For hydrogen alone, whether the escape occurs by Jeans escape or by blow-off makes little difference. The limiting factor is probably in the ultimate supply of hydrogen atoms and diffusion through the atmosphere (Hunten 1973). Perhaps the most appealing feature of the blow-off mechanism is that it may not be as selective as Jeans escape in discriminating against heavy atoms like sodium (Gross 1972). We will return to this point when we discuss the escape of sodium atoms.

VII. IO AS A SOURCE OF SODIUM

The observations of sodium emission in Region *B* reveal that the cloud is remarkably stable (Bergstralh *et al* 1975) and that solar resonant scattering is probably the excitation mechanism. This suggests that if Io were the source of sodium the required escape rate would be of order 10^7 atoms cm^{-2}

sec^{-1} (McElroy and Yung 1975; Macy and Trafton 1975). This deduction is based on an estimated population of 10^{30} sodium atoms and a photoionization lifetime of 10^6 sec (Hunten 1954). Comparison with Sec. VI shows that the estimated sodium source is four orders of magnitude smaller than the hydrogen source; the hydrogen atoms are approximately 10^3 times more numerous in Region *B*, and they are depleted about 10 times faster.

In the following subsections A and B we discuss two possible sources for sodium in the atmosphere of Io, namely sputtering from the surface and a meteoritic source. In Sec. C we shall discuss escape processes which can move this sodium into Region *B* where it is observed. In Sec. D we comment briefly on the significance of the absence of other metallic emission lines.

A. Sputtering

It is difficult to release sodium from the surface since metallic sodium as well as most common sodium compounds have low vapor pressures at Io's surface temperature ($\sim$ 140°K). Matson *et al.* (1974) proposed a sputtering mechanism involving the energetic particles in the Jovian magnetosphere. To date, this mechanism is the only plausible means we know for ejecting sodium from the surface into the atmosphere, but there are a number of difficulties, most of which have been discussed by Matson *et al.* (1974). The first potential problem is the presence of an atmosphere which may attenuate the influx of energetic particles. If the surface density of the neutral atmosphere is 10^{10} cm^{-3} and its scale height is 100 km, it will only be thin for interactions having cross-sections smaller than about 10^{-17} cm^2. Since that is approximately the cross-section for a one-MeV proton collision with a molecule, high energy protons probably reach the surface without substantial attenuation. The second problem is to have an adequate number of incident particles. In the keV – MeV range, the measured proton flux falls short of that required by more than an order of magnitude. It is conceivable that an "avalanche" process discussed by Matson *et al.* (1974) could remedy this deficiency, and we expect detailed models to carry this idea further.

B. Meteoritic Source

A number of papers (Morrison and Cruikshank 1974; Mekler *et al.* 1975; Sill 1974) have suggested meteoritic material as the source of Io's sodium. This idea is largely motivated by our understanding of the terrestrial sodium emission. Hunten and Wallace (1967) and Donahue and Meier (1967) first suggested that the origin of Earth's sodium atoms could be connected to the presence of dust. Possible mechanisms for releasing the sodium atoms include meteoric ablation (Gadsden 1968) and sublimation of dust particles (Fiocco and Visconti 1973; Fiocco *et al.* 1974).

Measurements of micrometeoroids in the Jovian environment by Pioneer 10 and 11 (Humes *et al.* 1974)[6] indicated that the mass flux of meteoroids

[6]See p. 1064.

intercepted by Io could be two orders of magnitude higher than that measured for Earth ($\sim 2 \times 10^{-16}$ g cm^{-2} sec^{-1}). Assuming a sodium concentration of 0.66% by weight, a value typical of chondritic meteorites (Junge *et al.* 1962), we estimate the net sodium source to be $\sim 3 \times 10^6$ atoms cm^{-2} sec^{-1}. The sodium atoms can be released from the meteorites by evaporation at the moment of impact or by sputtering after the material has settled down on the surface. The first mechanism faces the difficulty of explaining why sodium has not been observed on any one of the other Galilean satellites. The second mechanism would suggest that the sodium content in the Jovian meteorites must be higher by at least a factor of 10 than that typical of chondritic meteorites. These difficulties must be answered by any future theory that seriously proposes a meteoritic origin of Io's sodium.

C. *Escape of Sodium*

While the atmosphere could be thin to the incident energetic particles, the discussion in Sec. V.E indicates that it probably appears thick to the sputtered atoms, which typically have an energy of a few eV and a cross-section of $\sim 10^{-15}$ cm^2. The sodium atoms are probably thermalized in the atmosphere. The meteoritic source also yields sodium only to the bound atmosphere, so an escape mechanism must be formulated. Jeans escape would require an exospheric temperature of order 10,000°K, which could be achieved sporadically (as described in Sec. VI.A). Matson *et al.* (1974) considered a solar wind-type interaction between the upper atmosphere and the magnetospheric protons. Since the sodium problem is probably related to that of the hydrogen, we can gain some insight by examining Io's hydrogen escape. Gross (1972) has shown that hydrogen in a moderately hot thermosphere is not stable against a blow-off (see Sec. VI.C). If a hydrogen blow-off occurs with sodium as a minor component, it is possible that sodium will be dragged along.

D. *Implications of Undetected Emissions*

The absence of other metallic emission lines is puzzling. Considerations of cosmic abundance, oscillator strength and solar radiation lead us to expect that a number of optical resonance lines, notably Ca (4227 Å), Al (3962 Å), K (7665 Å), could have intensities comparable to those of the sodium D-lines. But as discussed in Sec. III, no other metallic lines have yet been identified, despite considerable effort devoted to the searches.

It is of interest to note a similar circumstance for the comets. The visible spectrum of Comet Mkros shows an extensive sodium emission, but no other metallic lines have been detected (Greenstein and Arpigny 1962). Greenstein and Arpigny considered their absence significant and drew attention to the difference in dissociation potentials of the oxides and hydrides of metals. In general, the dissociation potential of the hydrides is low, e.g., 2.2 eV for NaH, < 2.5 eV for MgH, < 3.1 eV for AlH, and < 1.7 eV for CaH. The oxides have higher dissociation potentials, e.g., 3.7 eV for MgO, < 3.7 eV

for AlO, and 5.9 eV for CaO. Therefore, if NaH were the parent molecule for atomic Na, it could easily be dissociated. But if CaO were the parent molecule for atomic Ca, it would not be dissociated as easily.

We may note the truly unique nature of sodium on Io. Not only is sodium the only metallic line detected so far, but Io is also the only one of the four Galilean satellites to possess this emission. It is difficult to think that a meteoritic source would favor a particular satellite or that sputtering by MeV protons would discriminate against other metallic atoms. It appears that the absence of other metallic emissions from Io and the absence of sodium emission from the other Galilean satellites could be used to provide useful constraints on the chemical nature of the surfaces of the Galilean satellites or on the mechanism for releasing the metallic atoms from their bound state.

VIII. SUMMARY

The current state of our knowledge of Io's atmosphere is summarized schematically in Fig. 16 which includes all the observational constraints. The quantities enclosed between brackets are hypothesized "missing links," advanced theoretically to complete the picture. We distinguish two types of models, characterized by the source for hydrogen. In the Type 1 Model, hydrogen is supplied by dissociation of ammonia. Proton charge exchange is the primary source of hydrogen in the Type 2 Model. Both models have the common feature that meteoritic impact or sputtering of the surface provides a source for sodium.

The main problem of the Type 1 Model is the need to free nitrogen at about the same rate as hydrogen. Thermal escape would require an exospheric temperature of order 10,000°K, a value in conflict with the implication in the ionosphere data of a temperature less than 1000°K. We are forced to conclude that the escape process is sporadic and was not operative during the Pioneer 10 encounter. On the other hand, the remarkable temporal stability of the sodium cloud implies that any sporadic process must occur with sufficient frequency so that the amount of sodium ejected each time is small compared with the total contents of Region *B*. This demand is not difficult to meet since the sodium cloud has a photoionization lifetime of about two weeks.

The main problem with the Type 2 Model is that the observed flux of charged particles is insufficient to supply the observed hydrogen cloud maintained in the steady state. The discrepancy is not considered serious since we have no observational evidence for the stability of the hydrogen cloud, and an abundant supply of low-energy protons below the threshold of the Pioneer detectors cannot be ruled out. This model opens up the attractive possibility of a relatively cold upper atmosphere as implied by the ionosphere measurement. Escape of hydrogen can be accomplished by Jeans

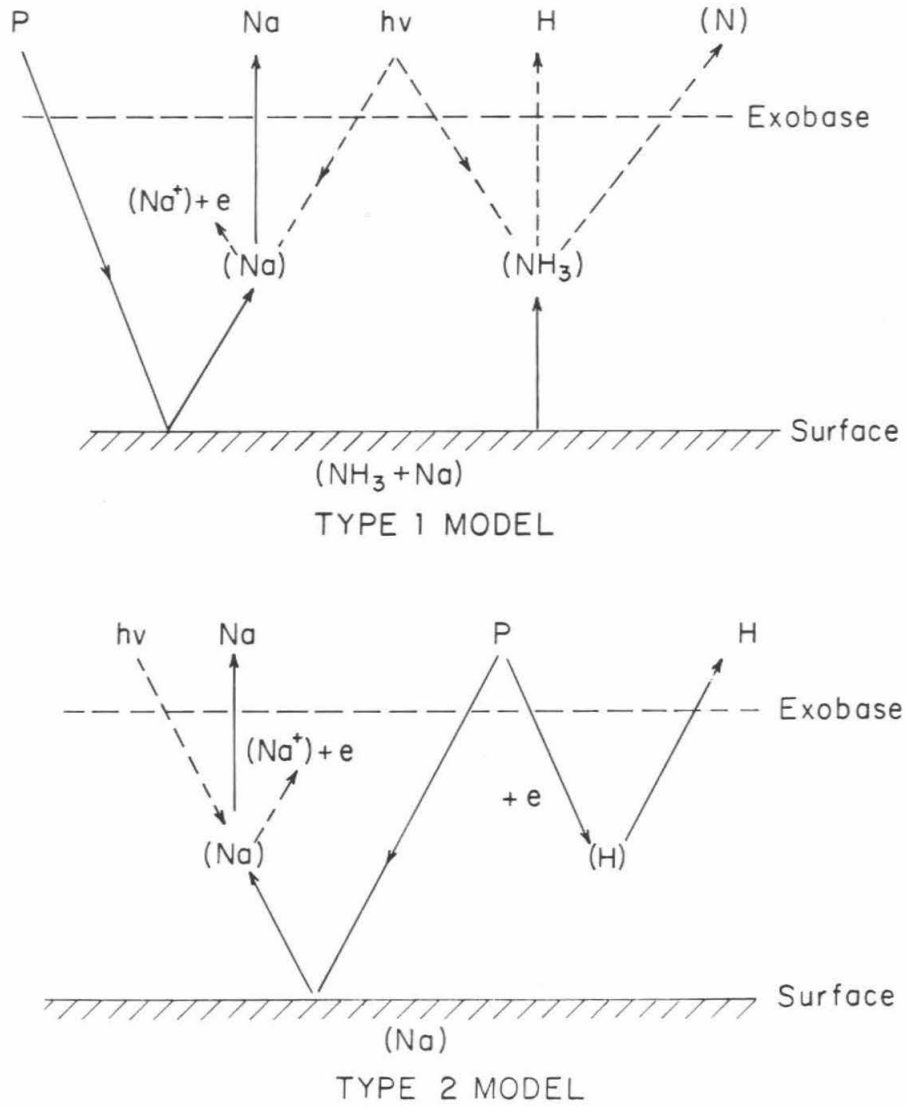

Fig. 16. Schematic diagram of Type 1 and Type 2 Models of Io's atmosphere.

escape of a blow-off process. The escape rate of sodium is many orders of magnitude lower than that of hydrogen. A blow-off will result in the loss of the entire exosphere, dragging away any minor species like sodium.

We note that within the context of present observational constraints, Type 1 Model is sporadic. The sporadic nature is crucially introduced to resolve the conflict between the high exospheric temperature (10,000°K) needed to free nitrogen (to a lesser extent, sodium) and the observed iono-

spheric temperature (~ 500°K). The Type 2 Model probably is sporadic too. The observed proton flux is not high enough to maintain the hydrogen cloud in a steady state. Escape of sodium depends on the sporadic blow-off of hydrogen from the upper atmosphere.

Acknowledgements. We are pleased to acknowledge many helpful discussions with our colleagues R. Goody, M. McElroy, F. Murcray, and W. Smyth. We thank R. Carlson, A. Eviatar, D. Hunten, D. Judge, D. Matson, M. Rosen, L. Trafton, and P. Wehinger for critical comments on the manuscript. This research was funded by the Atmospheric Sciences Section of the National Science Foundation under grant DES72-01472 A03 to Harvard University. One of us (Yuk L. Yung) acknowledges support by Kitt Peak National Observatory under NASA Contract NAS7-100.

DISCUSSION

D. M. Hunten: Meteoroid evaporation is usually considered to be the source of mesospheric sodium on Earth. Also, we should not be too literal about relative abundances. Several of the atoms one would expect to see are not found in terrestrial twilight, and we do not understand the selectivity. There seems to be something special about sodium that keeps it in the atomic form so that it is readily detected.

R. W. Carlson: The probable loss mechanism for the sodium atoms is ionization by electrons in the thermal plasma. Frank *et al.* have analyzed data from the Plasma Analyzer Experiment on Pioneer 10 and find densities of ~ 50 cm^{-3} at the orbit of Io, with an ion temperature of ~ 100 eV. Assuming that the electron and ion temperatures are the same, and using the ionization cross section of Na, they find a lifetime of ~ 10^5 sec, roughly an order of magnitude shorter than the photoionization lifetime.

L. Trafton: Io's cloud sometimes exhibits sodium profiles with a high degree of asymmetry. These suggest that macroscopic motion is important. This implies that temperatures of about 5000°K, that you derive from the line widths, may be excessive. Also, a large column abundance of sodium can cause the line to appear broad at low temperatures because of saturation.

D. L. Matson: The key question about Io's atmosphere is its pressure. This quantity is poorly known because the currently available values are model dependent. The variety of models which have been considered do not include all of the physical processes which are known to occur at Io. For example, the field and forces due to the plasma sheaths have not yet been considered.

REFERENCES

Allen, C. W. 1973. *Astrophysical Quantities*. London: The Athlone Press.

Anderson, J. D.; Null, G. W.; and Wong, S. K. 1974. Gravity results from Pioneer 10 Doppler data. *J. Geophys. Res.* 79:3661–3664.

Barmore, F. E. 1975. The filling-in of Fraunhofer lines in the day sky. *J. Atmos. Sci.* 32:1489–1493.

Bauer, S. J. 1973. *Physics of planetary ionospheres*. New York: Springer Verlag.

Bergstralh, J. T.; Matson, D. L.; and Johnson, T. V. 1975. Sodium D-line emission from Io: synoptic observations from Table Mountain Observatory. *Astrophys. J.* 195:L131–L135.

Bigg, E. K. 1964. Influence of the Satellite Io on Jupiter's decametric emission. *Nature* 203: 1008–1010.

Binder, A. B., and Cruikshank, D. P. 1964. Evidence for an atmosphere on Io. *Icarus* 3:299–305.

Blamont, J. E., and Courtès, G. 1955. Noveau procédé d'étude photométrique des émissions monochromatiques du ciel nocturne. *Ann. Géophys.* 11:252–254.

Brown, R. A. 1974. Optical line emission from Io. *Exploration of the planetary system*. (A. Woszczyk and C. Iwaniszewska, eds.) pp. 527–531. Dordrecht, Holland: D. Reidel Publ. Co.

Brown, R. A., and Chaffee, F. H. 1974. High-resolution spectra of sodium emission from Io. *Astrophys. J.* 187:L125–L126.

Brown, R. A.; Goody, R. M.; Murcray, F. J.; and Chaffee, F. H. 1975. Further studies of line emission from Io. *Astrophys. J.* 200:L49–L53.

Carlson, R. W., and Judge, D. L. 1974. Pioneer 10 ultraviolet photometer observations at Jupiter encounter. *J. Geophys. Res.* 79:3623–3633.

———. 1975. Pioneer 10 ultraviolet photometer observations of the Jovian hydrogen torus: the angular distribution. *Icarus* 24:395–399.

Chamberlain, J. W. 1961. *Physics of the aurora and airglow*. New York: Academic Press.

———. 1965. Planetary coronae and atmospheric evaporation. *Planet. Space Sci.* 11:901–960.

Cloutier, P. A.; McElroy, M. G.; and Michel, F. C. 1969. Modifications of the Martian ionosphere by the solar wind. *J. Geophys. Res.* 74:6215–6228.

Cruikshank, D. P.; Pilcher, C. B.; and Sinton, W. M. 1974. Io: reported helium emission. *IAU Circular* Nos. 2693 and 2722.

Donahue, T. M., and Meier, R. R. 1967. Distribution of sodium in the daytime upper atmosphere as measured by a rocket experiment. *J. Geophys. Res.* 72:2803–2829.

Fanale, F. P.; Johnson, T. V.; and Matson, D. L. 1976. Io's surface and the histories of the Galilean satellites. *Planetary Satellites*. (J. Burns, ed.) Tucson: Univ. of Arizona Press.

Fanale, F. P.; Nash, D. B.; Johnson, T. V.; and Matson, D. L. 1975. The surface of Io: a progress report. *Bull. Amer. Astron. Soc.* 7:386.

Fink, U.; Dekkers, N. H.; and Larson, H. P. 1973. Infrared spectra of the Galilean satellites of Jupiter. *Astrophys. J.* 179:L155–L159.

Fiocco, G.; Fua, E.; and Visconti, G. 1974. Origin of the upper atmospheric Na from sublimating dust: a model. *Ann. Géophys.* 30:517–528.

Fiocco, G., and Visconti, G. 1973. On the seasonal variation of upper atmospheric sodium. *J. Atm. Terr. Phys.* 35:165–171.

Frank, L. A.; Ackerson, K. L.; Wolfe, J. H.; and Mihalov, J. D. 1975. Observations of plasmas in the Jovian magnetosphere. *J. Geophys. Res.* 81:457–468.

Gadsden, M. 1968. Sodium in the upper atmosphere: meteoric origin. *J. Atm. Terr. Phys.* 30: 151–161.

Goldreich, P., and Lynden-Bell, D. 1969. Io, a Jovian unipolar inductor. *Astrophys. J.* 156: 59–78.

Greenstein, J. L., and Arpigny, C. 1962. The visual region of the spectrum of comet Mkros (1957d) at high resolution. *Astrophys. J.* 135:892–905.

Gross, S. H. 1972. On the exospheric temperature of hydrogen dominated planetary atmospheres. *J. Atmos. Sci.* 29:214–218.

———. 1974. The atmospheres of Titan and the Galilean satellites. *J. Atmos. Sci.* 31:1413–1420.

Humes, D. H.; Alvarez, J. M.; O'Neal, R. L.; and Kinard, W. H. 1974. The interplanetary and near-Jupiter meteoroid environments. *J. Geophys. Res.* 79:3677–3684.

Hunten, D. M. 1954. A study of sodium in twilight. I. theory. *J. Atmos. Terr. Phys.* 5:44–56.

———. 1965. Excitation of the sodium emission in aurora. *J. Atm. Terr. Phys.* 27:583–586.

———. 1973. The escape of H_2 from Titan. *J. Atmos. Sci.* 30:726–732.

Hunten, D. M., and Wallace, L. 1967. Rocket measurement of the sodium dayglow. *J. Geophys. Res.* 72:69–79.

Johnson, T. V., and McCord, T. B. 1970. Galilean satellites: the spectral reflectivity 0.30-1.10 micron. *Icarus* 13:37–42.

Judge, D. L., and Carlson, R. W. 1974. Pioneer 10 observations of the ultraviolet glow in the vicinity of Jupiter. *Science* 183:317–318.

Junge, C. E.; Oldenberg, O.; and Wasson, J. T. 1962. On the origin of the sodium present in the upper atmosphere. *J. Geophys. Res.* 67:1027–1039.

Kliore, A.; Cain, D. L.; Levy, G. S.; Eshleman, V. R.; Fjeldbo, G.; and Drake, F. D. 1965. Occultation experiment: results of first direct measurement of Mars's atmosphere and ionosphere. *Science* 149:1243–1248.

Kliore, A.; Fjeldbo, G.; Seidel, B. L.; Sweetnam, D. N.; Sesplaukis, T. T.; and Woiceshyn, P. M. 1975. Atmosphere of Io from Pioneer 10 radio occultation measurements. *Icarus* 24: 407–410.

Kliore, A.; Levy, G. S.; Cain, D. L.; Fjeldbo, G.; and Rasool, S. I. 1967. Atmosphere and ionosphere of Venus from Mariner V S-Band radio occultation measurement. *Science* 158: 1683–1688.

Macy, W., and Trafton, L. 1975. A model for Io's atmosphere and sodium cloud. *Astrophys. J.* 200:510–519.

Matson, D. L.; Johnson, T. V.; and Fanale, F. P. 1974. Sodium D-line emission from Io: sputtering and resonant scattering hypothesis. *Astrophys. J.* 192:L43–L46.

McDonough, T. R. 1975. A theory of the Jovian hydrogen torus. *Icarus* 24:400–406.

McElroy, M. B., and Yung, Y. L. 1975. The atmosphere and ionosphere of Io. *Astrophys. J.* 196:227–250.

McElroy, M. B.; Yung, Y. L.; and Brown, R. A. 1974. Sodium emission from Io: implications. *Astrophys. J.* 187:L127–L130.

Mekler, Yu., and Eviatar, A. 1974. Spectroscopic observations of Io. *Astrophys. J.* 193:L151–L152.

Mekler, Yu.; Eviatar, A.; and Coroniti, F. V. 1975. Sodium in the Jovian atmosphere. *Astrophys. Space Sci.* In draft.

Mertz, L. 1975. Heterographic techniques for astronomy. Paper delivered at OSA Meeting, "Imaging in Astronomy." Cambridge, Massachusetts, June 18–21, 1975.

Morrison, D., and Cruikshank, D. P. 1974. Physical properties of the natural satellites. *Space Sci. Rev.* 15:641–739.

Morrison, D., and Morrison, N. D. 1976. Photometry of the Galilean satellites. *Planetary Satellites.* (J. Burns, ed.) Tucson: Univ. of Arizona Press.

Münch, G., and Bergstralh, J. T. 1975. Sodium D-line emission from Io: spatial brightness distribution from multislit spectra. *Bull. Am. Astron. Soc.* 7:386.

Öpik, E. J. 1963. Selective escape of gases. *Geophys. J.* 7:490–509.

Parker, E. N. 1958. Dynamics of the interplanetary gas and magnetic fields. *Astrophys. J.* 128:664–675.

Parkinson, T. D. 1975. Excitation of the sodium D-line emission observed in the vicinity of Io. *J. Atmos. Sci.* 32:630–633.

Pilcher, C. B.; Ridgway, S. T.; and McCord, T. B. 1972. Galilean satellites: identification of water frost. *Science* 178:1087–1089.

Shawhan, S. D. 1976. Io sheath-accelerated electrons and ions. *Icarus* (special Jupiter issue). In press.

Shawhan, S. D.; Goertz, C. K.; Hubbard, R. F.; Gurnett, D. A.; and Joyce, G. 1974. Io: accelerated electrons and ions. Paper presented at Neil Brice Memorial Symposium, *The magnetosphere of the earth and Jupiter*, May, 1974, Frascati, Italy.

Sill, G. T. 1974. Sources of sodium in the atmosphere of Io. *Bull. Am. Astron. Soc.* 6:384.

Smith, B. A., and Smith, S. A. 1972. Upper limits for an atmosphere on Io. *Icarus* 17:218–222.

Taylor, G. E.; O'Leary, B.; Van Flandern, T. C.; Bartholdi, P.; Owen, F.; Hubbard, W. B.; Smith, B. A.; Smith, S. A.; Fallon, F. W.; Devinney, E. J.; and Oliver, J. 1971. The occultation of Beta Scorpii C by Io on May 14, 1971. *Nature* 234:405–406.

Trafton, L. 1976. A search for emission features in Io's extended cloud. *Icarus* (special Jupiter issue). In press.

Trafton, L., and Macy, W. 1975. The geometry of Io's sodium cloud. *Bull. Am. Astron. Soc.* 7:386.

Trafton, L.; Parkinson, T.; and Macy, W. 1974. The spatial extent of sodium emission around Io. *Astrophys. J.* 190:L85–L89.

Webster, D. L.; Alksne, A. Y.; and Whitten, R. C. 1972. Does Io's ionosphere influence Jupiter's radio bursts? *Astrophys. J.* 174:685–696.

Wehinger, P., and Wyckoff, S. 1974. Jupiter I. *IAU Circular No. 2701.*

Wehinger, P. A.; Wyckoff, S.; and Frohlich, A. 1976. Mapping of the sodium emission associated with Io and Jupiter. *Icarus* (special Jupiter issue). In press.

Whitten, R. C.; Reynolds, R. T.; and Michelson, P. F. 1975. The ionosphere and atmosphere of Io. *Geophys. Res. Lett.* 2:49–51.